THE UNIVERSITY OF ALBERTA

RELEASE FORM

NAME OF AUTHOR DOO - PYO HONG

TITLE OF THESIS OPTIMAL JUMP NONHOMOGENEITY OF A BAR IN SAINT-VENANT TORSION

DEGREE FOR WHICH THESIS WAS PRESENTED MASTER OF SCIENCE

YEAR THIS DEGREE GRANTED FALL 1980

THE UNIVERSITY OF ALBERTA

OPTIMAL JUMP NONHOMOGENEITY OF A BAR IN SAINT-VENANT TORSION

by

© DOO - PYO HONG

A THESIS

SUBMITTED TO THE FACULTY OF GRADUATE STUDIES AND RESEARCH

IN PARTIAL FULFILMENT OF THE REQUIREMENTS FOR THE DEGREE

OF MASTER OF SCIENCE

MECHANICAL ENGINEERING

EDMONTON, ALBERTA

FALL 1980

THE UNIVERSITY OF ALBERTA

FACULTY OF GRADUATE STUDIES AND RESEARCH

The undersigned certify that they have read, and recommend to the Faculty of Graduate Studies and Research, for acceptance, a thesis entitled OPTIMAL JUMP NONHOMOGENEITY OF A BAR IN SAINT-VENANT TORSION submitted by DOO - PYO HONG in partial fulfilment of the requirements for the degree of MASTER OF SCIENCE.

Doo - Pyo Hong
6411 - 35 Ave.,
Edmonton, Alberta
Canada T6L 1G5

Drs. M.G.Faulkner & A.Mioduchowski
Dept. of Mechanical Engineering
University of Alberta
Edmonton, Alberta
Canada

Dear Dr.M.G.Faulkner and Dr.A.Mioduchowski

By considering an optimization problem of nonhomogeneous bars subjected to Saint-Venant torsion as a variational problem, a necessary optimality condition is derived and thus an iterative procedure is established based on the derived condition. This simple iterative procedure combined with the Finite Element Method (Hybrid stress approach) is applicable to the bars with different cross-sections other than a square, although only the square cross-section is considered in this study.

From the computation results performed by the AMDAHL 470V/6 in the Computing Service, University of Alberta, it is found that the optimal solution in this case where the shear modulus function varies jump-like behaves similarly with that in which the material constant varies continuously. It is further observed that the improvement in the torsional rigidity by optimization is more significant for a square bar than for a circular bar.

Hoping that you find this thesis satisfactory,

Yours truly,

ABSTRACT

The growing interest over the use of composite material systems makes it important to study the problem of optimal nonhomogeneity of a linearly-elastic bar in torsion. This is a basic example of the problem of finding the most efficient use of material in such systems.

The optimization problem is formulated as a variational problem in order to derive the necessary conditions for optimality. In this formulation, the shear modulus function whose values take either of two different shear moduli G or G , is accepted as a control function to be optimized, while the proportion of reinforcement p is specified as a constraint.

For the given material constants G_1, G_2 and a given proportion of reinforcement p, the iteration procedure is carried out by the computer program to achieve the maximum (or minimum) torsional rigidity. The computer program uses the Constant Strain Triangle Finite Element Method formulated on the basis of the hybrid stress approach for calculating the stress solution of torsion.

A square, prismatic bar of unit length is taken for a test analysis to demonstrate the correctness and accuracy of the computer program. The test results show that the optimal solution is unique and convergent in the practical sense.

Numerical analysis is then carried out for a square bar with different shear modulus ratios and with various

proportions of reinforcement. The results are presented and compared with the known solutions for a bar with circular cross-section. These analytical results show that a square bar can be more efficiently optimized than a circular bar.

It is believed that the present study may find applications in other fields such as structures, heat transfer and seepages.

ACKNOWLEDGEMENT

The author would like to express his deep appreciation to Dr.M.G.Faulkner and Dr.A.Mioduchowski, who both supervised this thesis, for their invaluable advice, guidance and suggestion of the topic. Thank is also due to his wife for her endless patience and encouragement.

Funding was partly provided by the National Research Council(NRC A7514).

NOMENCLATURE

A	area of a cross-section
A_1, A_2	areas of zones of material *1* and *2*
a	radius of a circular cross-section
a_i, a_j, a_k	$a_i = x_k - x_j$ in cyclic order of i, j and k
b	radius of inner circle
C	boundary of a cross-section
eff.	efficiency of optimization
$G, G(x,y)$	shear modulus function
G_1, G_2	shear moduli of two different materials
J	torsional rigidity
J_1, J_2, J_{op}	torsional rigidities of G_1-homogeneous, G_2-homogeneous and optimal nonhomogeneous bars
l	a side of a square cross-section
M	twisting moment
n	number of nodal points
p	proportion of reinforcement
R	cross-section of a bar
U	strain energy
$u, u(x,y)$	specific compliance, which is inverse of shear modulus function
u_1, u_2	specific compliances of two materials
v_x, v_y, v_z	dispalcements in x, y and z direction, respectively
W	potential of the surface tractions
x, y, z	rectangular coordinates
η	admissible functions

θ	twist angle per unit length
τ	shear stress
π	complementary energy
$\phi, \phi(x,y)$	Prandtl's stress function
$\psi, \psi(x,y)$	warping function

Subscripts

i,j,k	three nodes of an element numbered counter-clockwise
$1,2$	two different materials
$r, r+1$	iteration steps

Table of Contents

List of Tables

List of Figures

1. INTRODUCTION

The torsion problem for a prismatic bar was correctly formulated by Saint-Venant[20],[1] who showed how the torsion problem fitted into the general theory of elasticity. According to Saint-Venant, the behavior of a prismatic bar can be approximated by considering only the behavior of a typical cross-section of the bar, and the twisting of the bar is composed of a rotation of this cross-section which is proportional to its distance from the origin and of a warping of the cross-section that is identical for all cross-sections.

The torsion function (warping function) which is a function of the planar coordinates only, is known to satisfy the two dimensional Laplace equation thus the torsion problem reduces to a Neumann-type problem. Alternatively, it is found that the torsion problem can be reduced to a Dirichlet-type problem by introducing Prandtl's stress function. The solutions for torsion problems in terms of these two functions allow the complete analysis in the case of a homogeneous, elastic bar. For all but certain cross-sections, an analytical solution may involve the use of Fourier series or complex variables.

However, even these cumbersome analytical solutions are not generally available for the cases of nonhomogeneous, irregular shape of cross-sections or bars in elastic-plastic deformation, due to the complexity of the analytical

---

[1] Numbers in square brackets refer to references.

procedure.

These more complicated torsion problems have been the object of many investigations using various techniques such as a graphical method for plastic materials[14,19] and finite difference[9] or direct numerical technique[4] for the elastic case.

The Finite Element Method was employed by Herrman[7] in solving torsion problems for irregular shapes. His work is based on the displacement formulation, in which the potential energy is expressed in terms of the assumed warping function, and its stationary value leads to approximate equilibrium equations. This warping function must be chosen such that it satisfies the compatibility relations.

In a series of achievements by Moan[15], Herakovich [5,6] and Hodge[5,8], the finite element stress formulation was used. Here, the stress function which satisfies equilibrium is substituted into the complementary energy, and its stationary value yields approximate compatibility equations. The choice of "the best" element is discussed in the work of Moan, while quadratic programming is used by Herakovich and Hodge in solving elastic-plastic torsion of hollow and nonhomogeneous bars.

For the assumed unknown functions in either the displacement or stress formulation, the equilibrium or the compatibility relations are satisfied only in an approximate sense. For example, in the case of the displacement

formulation, the stress boundary condition that the normal component of the stress along the boundary of the cross-section vanishes is not necessarily satisfied; while in the case of stress formulation, the warping is not continuous over the cross-section especially in the case of a nonhomogeneous bar. In fact, the nonhomogeneous bar studied in the work of Herakovich[6] is not truly nonhomogeneous - the two materials have different yield limits, but the elastic shear modulus is constant throughout the cross-section of the bar, that is, the bar is nonhomogeneous only for plastic deformation.

In order to overcome some of the deficiencies of both the displacement and stress formulation, the hybrid approach was first introduced by Pian[18] and developed further by Yamada et al.[22]. A number of variations are available with the hybrid approach, however the torsion solutions for nonhomogeneous bars can be improved by assuming a stress distribution inside the element and the displacements on the boundaries of the element so that all of the equilibrium, compatibility and stress boundary conditions can be satisfied.

In an alternate mixed approach which was recently presented by Noor and Anderson[17], both the displacement and stress functions are assumed inside the element and on the boundaries of the element as well. The solutions obtained by this approach are much improved, but the number of equations for the same number of elements is larger than

that which occurs in the displacement, stress or hybrid approaches. As a result of these considerations, the solution in this work uses the hybrid stress approach.

Due to the recent interest in the development of efficient composite material systems, the torsion problem for nonhomogeneous bars has received renewed consideration as an optimal design problem. The mathematical formulation of the problem of finding the optimal control function (shear modulus function in this case) when the state equation is expressed in a partial differential form is due to Cea and Malanowski[2], In their work, it is shown that the solution of this type of problem exists and is unique and that a convergent iterative algorithm can be constructed to find the optimal solution.

Klosowicz and Lurie[10] developed the idea of Cea and Malanowski further by employing a Lagrange multiplier and thus obtained a similar algorithm to that described in [2]. Klosowicz[9] then carried out the iteration by using the finite diffference technique for solving the state equation at every step of the iteration, and finally obtained the solutions for square and elliptic bar cross-sections. It was revealed by his study that 'the rigid reinforcement should be located near the center of the lateral surfaces of the bar when the weak material prevails while with increasing amount of stiffer material the configuration of the reinforcement must change to form a belt around the center of the cross-section'.

For this same purpose, Banichuk[1] used a perturbation technique to find the optimizing shape of cross-section instead of optimizing the shear modulus distribution within the given cross-section. Among all the cross-sections of the same area, it was shown that the anisotropic bar with maximum torsional rigidity had an elliptic shape,

The optimal nonhomogeneity in torsion for perfectly plastic bars (yield limit was the control function) was considered by Mioduchowski[13,14]. He employed the method of incomplete gradient and local variation on prismatic bars with square, circular and elliptic cross-sections. His study revealed that 'for solutions ensuring maximum load carrying capacity, zones of higher yield limit occur in regions where plastic zones would first occur in a homogeneous bar of the same cross-section'. It was further shown that 'the zones of higher yield limit form around the center of the lateral surfaces when the difference between two material constants is small while with increasing difference the zones change to form a belt shape around the center of the cross-section'. These conclusions are remarkably similar to those presented by Klosowicz[9].

It should be mentioned here that in the works of Klosowicz and Mioduchowski, the control function (either the shear modulus or yield limit function) is assumed continuous over the cross-section such as might occur during a mechanical or heat treatment of the bar. It is however almost impossible by this means to obtain a desired

distribution of material constants. Furthermore, it is unlikely that the average shear modulus or yield limit has any significance for practical engineering problems.

In the present investigation, the problem of optimization of the same nature as found in [2] and [9,10] is studied. However the shear modulus in this problem varies in a jump-like manner which often occurs in practice when a bar is composed of prismatic parts of two completely different materials.

The proportion of reinforcement instead of the average shear modulus is prescribed as a constraint and the optimizing step function of shear modulus which satisfies all the state equation, boundary conditions and the constraint will be sought. The iterative algorithm constructed for this purpose is very simple and easy compared with those found in [2] and [10].

This study considers only the linearly-elastic behavior of the bars, however, it is believed that the perfectly plastic behavior would be similar.

2. FORMULATION OF THE PROBLEM

2.1 Saint-Venant Torsion

A general solid prismatic bar which is subjected to torsion is shown in Figure 2.1. Under the assumptions of Saint-Venant for bars of this type, each cross-section warps the same way and each rotates by an angle proportonal to its distance from the origin with no in-plane distortion. This is expressed analytically by

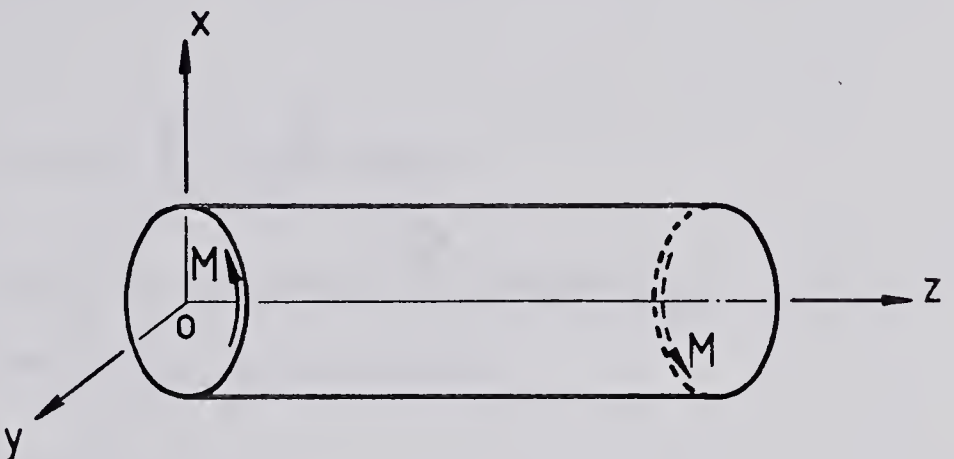

Fig. 2.1 Coordinate system of a prismatic bar

$$
\begin{aligned}
v_x &= -\theta yz, \\
v_y &= \theta zx, \qquad (2.1) \\
v_z &= \theta \psi(x,y).
\end{aligned}
$$

where ψ defines the warping and is a function of x and y alone, and θ is the angle of twist per unit length.

The only nonvanishing stress components are derived by the stress-strain law as

$$
\begin{aligned}
\tau_{zx} &= G\theta\left(\frac{\partial \psi}{\partial x} - y\right), \\
\tau_{zy} &= G\theta\left(\frac{\partial \psi}{\partial y} + x\right). \qquad (2.2)
\end{aligned}
$$

A substitution of these values into the equations of equilibrium yields the Laplace equation as

$$(2.3) \qquad grad^2\psi = \frac{\partial^2\psi}{\partial x^2} + \frac{\partial^2\psi}{\partial y^2} = 0.$$

The boundary condition of the traction-free lateral surface yields

$$(2.4) \qquad (\frac{\partial\psi}{\partial x}-y)\frac{dy}{ds}-(\frac{\partial\psi}{\partial y}+x)\frac{dx}{ds} = 0,$$

while the shear stresses on the ends result in a twisting moment as

$$(2.5) \qquad M = G\theta\iint_R (x^2+y^2+x\frac{\partial\psi}{\partial y} -y\frac{\partial\psi}{\partial x})dxdy.$$

The Prandtl's stress function ϕ is defined in terms of warping function or the shear stresses by

$$(2.6) \qquad \begin{aligned} \frac{\partial\phi}{\partial y} &= T_{zx} = G\theta(\frac{\partial\psi}{\partial x}-y), \\ \frac{\partial\phi}{\partial x} &= -T_{zy} = -G\theta(\frac{\partial\psi}{\partial y}+x). \end{aligned}$$

With this definition, the torsion problem reduces to a Dirichlet-type problem of finding a function $\phi(x,y)$ which satisfies

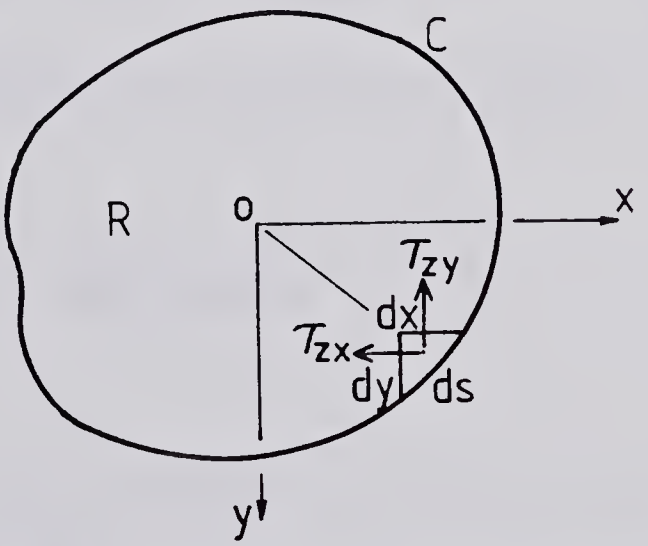

Fig. 2.2 Shear stresses on a cross-section

$$(2.7) \qquad grad^2\phi = -2G\theta \quad \text{in } R,$$

and the boundary condition on the lateral surface

$$(2.8) \qquad \phi = 0 \quad \text{on } C.$$

The expression for the twisting moment in terms of ϕ is then

$$(2.9) \qquad M = 2\iint_R \phi \, dxdy.$$

It can be shown that these two formulations above are derived from the principles of minimum potential energy and of minimum complementary energy. The formulation in the present study will be based on the latter which states: 'Among all the sets of admissible stresses that satisfy the equations of equilibrium and the boundary conditions, the set of actual stress components makes the total complementary energy an absolute minimum'.

The complementary energy is expressed in terms of the stress function as

$$(2.10) \qquad \pi_c = \iint_R \frac{1}{2G}\left[\left(\frac{\partial \phi}{\partial x}\right)^2 + \left(\frac{\partial \phi}{\partial y}\right)^2\right] dxdy - 2\theta \iint_R \phi \, dxdy.$$

The solution ϕ which minimizes π_c is also the unique solution of

$$(2.11) \qquad \iint_R \frac{1}{G} \, grad\,\phi \cdot grad\,\eta \, dxdy = 2\theta \iint_R \eta \, dxdy$$

for all admissible η.

Here, $grad\,\phi \cdot grad\,\eta$ denotes the scalar product of two vectors

$$(2.12) \qquad grad\,\phi \cdot grad\,\eta = \frac{\partial \phi}{\partial x}\frac{\partial \eta}{\partial x} + \frac{\partial \phi}{\partial y}\frac{\partial \eta}{\partial y}$$

and the admissible function η is in the class of functions that are continuous over the cross-section and satisfy the boundary conditions

(2.13) $\eta = 0$ on C.

It can be easily shown that eq.(2.11) is equivalent to the compatibility equation. Consider the LHS functional in eq.(2.11)

$$(2.14) \qquad \iint_R \frac{1}{G} \operatorname{grad}\phi \cdot \operatorname{grad}\eta \, dxdy$$
$$= \iint_R \frac{1}{G} \left(\frac{\partial \phi}{\partial x} \frac{\partial \eta}{\partial x} + \frac{\partial \phi}{\partial y} \frac{\partial \eta}{\partial y} \right) dxdy .$$

Taking the eq.(2.13) into consideration, this can be integrated as

$$(2.15) \qquad \iint_R \frac{1}{G} \left(- \frac{\partial^2 \phi}{\partial x^2} - \frac{\partial^2 \phi}{\partial y^2} \right) \eta \, dxdy .$$

Substitution of eq.(2.7) into eq.(2.15) finally yields

$$(2.16) \qquad \iint_R \frac{1}{G} (2G\theta) \eta \, dxdy = 2\theta \iint_R \eta \, dxdy$$

for all admissible η.

It is sometimes more convenient to use the eq.(2.11) for the purpose of theoretical developments and proofs. The formulation in the next section employs both of eqs.(2.10) and (2.11).

2.2 Formulation of the Optimization Problem

Figure 2.3 illustrates a nonhomogeneous, prismatic bar composed of a few prismatic components but made of two different materials of shear moduli G_1 and G_2. The problem is to find the optimal distribution of those components such that the maximum torsional rigidity can be achieved. The procedure followed is similar to that of Klosowicz and Lurie[10].

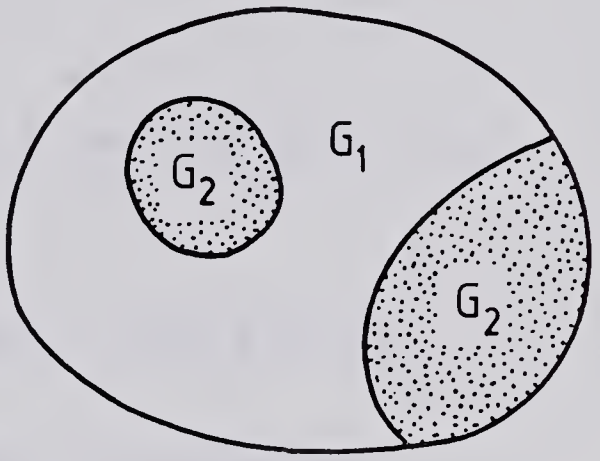

Fig. 2.3 Cross-section of a nonhomogeneous bar

The nonhomogeneity of the bar is described by the shear modulus function

$$(2.17) \qquad G(x,y) = \begin{cases} G_1 \text{ in Region } 1 \\ G_2 \text{ in Region } 2. \end{cases}$$

Here, it is assumed that

$$(2.18) \qquad 0 \le G_1 \le G_2.$$

The proportion of reinforcement is prescribed as a constraint

$$(2.19) \qquad p = \frac{A_2}{A}$$

where A, A_1 and A_2 denote the areas of the cross-section, region *1* and region *2*, respectively.

The objective is to achieve the maximum torsional rigidity or the maximum twisting moment for a given angle of twist

$$(2.20) \qquad M = 2\iint_R \phi \, dxdy.$$

This Prandtl's stress function ϕ must minimize the complementary energy

$$(2.21) \qquad \pi_c = \frac{1}{2}\iint_R \frac{1}{G}(grad\phi)^2 dxdy - 2\theta\iint_R \phi \, dxdy.$$

If the specific compliance is defined as

$$(2.22) \qquad u(x,y) = \frac{1}{G(x,y)},$$

then eq.(2.21) can be rewritten as

$$(2.23) \qquad \pi_c = \frac{1}{2}\iint_R u\,(grad\phi)^2 dxdy - 2\theta\iint_R \phi \, dxdy.$$

The stress function in eq.(2.23) is the unique solution of

$$(2.24) \qquad \iint_R u \; grad\phi \cdot grad\,\eta \, dxdy = 2\theta\iint_R \eta dxdy$$

for all admissible η.

If $\phi = \eta$ then

$$(2.25) \qquad \frac{1}{2}\iint_R u\,(grad\phi)^2 dxdy - 2\theta\iint_R \phi \, dxdy$$

$$= -\theta\iint_R \phi \, dxdy$$

Hence the problem can be stated as

$$(2.26) \qquad \max_{u,\phi}\ \theta \iint_R \phi\, dxdy.$$

where u and satisfy eq.(2.24) with the constraints

$$(2.27) \qquad u(x,y) = \begin{cases} u_1 & \text{in Region } 1 \\ u_2 & \text{in Region } 2 \end{cases}$$

where

$$(2.28) \qquad 0 \le u_2 \le u_1 .$$

3. SOLUTION PROCEDURE

3.1 Necessary Conditions for Optimality

The solution for the problem stated in the previous chapter does not appear possible by analytical means. However, since the objective of the present study is to develop a simple and versatile method which is applicable to any shape of cross-sections, the F.E.M. was used in conjunction with an iterative procedure.

Although no formal proof of sufficient and necessary conditions as well as the existence and convergence of the solution has been developed, these are accomplished in the practical manner in the next chapters.

In order to develop an iterative algorithm consider the functions u_r and ϕ_r are computed and u_{r+1} and ϕ_{r+1} in the next iteration are to be computed.

If

$$(3.1) \qquad \begin{aligned} u_{r+1} &= u_r + \Delta u_r \\ \phi_{r+1} &= \phi_r + \Delta \phi_r , \end{aligned}$$

then the objective functional for the r+1-th step becomes

$$(3.2) \qquad \begin{aligned} J_{r+1} &= \iint_R (u_r+\Delta u_r)\{grad(\phi_r+\Delta\phi_r)\}^2 dxdy \\ &= 2\theta \iint_R (\phi_r+\Delta\phi_r) dxdy . \end{aligned}$$

But since

$$(3.3)\qquad \iint_R (u_r+\Delta u_r)\,grad(\phi_r+\Delta\phi_r)\cdot grad\,\eta\,dxdy$$

$$= 2\theta\iint_R \eta dxdy$$

$$= \iint_R u_r\,grad\phi_r\cdot grad\,\eta\,dxdy,$$

for all admissible η,

the functional in eq.(3.2) can be expressed as

$$(3.4)\qquad J_{r+1} = \iint_R u_r\,grad\phi_r\cdot grad(\phi_r+\Delta\phi_r)\,dxdy$$

$$= J_r+\iint_R u_r\,grad\phi_r\cdot grad\Delta\phi_r\,dxdy.$$

Again from the identity eq.(2.24)

$$(3.5)\qquad \iint_R u_{r+1}\,grad(\phi_r+\Delta\phi_r)\cdot grad\phi_r\,dxdy$$

$$= 2\theta\iint_R \phi_r\,dxdy$$

$$= \iint_R u_r(grad\phi_r)^2 dxdy,$$

the relationship is obtained as

$$(3.6)\qquad \iint_R u_r\,grad\phi_r\cdot grad\Delta\phi_r\,dxdy$$

$$+\iint_R \Delta u_r\,grad(\phi_r+\Delta\phi_r)\cdot grad\phi_r dxdy$$

$$= 0.$$

By substitution of eq.(3.6) into eq.(3.4), the objective functional finally becomes

$$(3.7)\qquad J_{r+1} = J_r - \iint_R \Delta u_r\,grad(\phi_r+\Delta\phi_r)\cdot grad\phi_r\,dxdy.$$

Therefore, the increase of the value of the functional can be expressed as

$$(3.8) \qquad \Delta J_r = -\iint_R \Delta u_r (grad\phi_r)^2 dxdy - \iint_R \Delta u_r grad\phi_r \cdot grad\Delta\phi_r dxdy.$$

If $grad\Delta\phi_r$ is negligible compared with $grad\phi_r$, ΔJ_r can be approximated as

$$(3.9) \qquad \Delta J_r \cong -\iint_R \Delta u_r (grad\phi_r)^2 dxdy.$$

The necessary conditions for achieving the maximum torsional rigidity is that ΔJ_r in eq.(3.9) should be positive, or

$$(3.10) \qquad \iint_R \Delta u_r (grad\phi_r)^2 dxdy < 0.$$

Consider a cross-section of a bar divided into a number of constant strain triangles - see Figure 3.1. And let u_{r+1} be different from u_r in the elements i and j alone, i.e.,

$$(3.11) \qquad \Delta u_r = \begin{cases} u_2 - u_1 & \text{in element } i \\ u_1 - u_2 & \text{in element } j \\ 0 & \text{elsewhere.} \end{cases}$$

The integration in eq.(3.10) can now be performed as

$$(3.12) \qquad \Delta J_r \cong (u_1 - u_2)\,[(grad\phi_r)^2_i - (grad\phi_r)^2_j]$$

Since $u_2 < u_1$ (or $G_1 < G_2$), ΔJ_r is positive when

(3.13) $$(grad\phi_r)^2_i > (grad\phi_r)^2_j$$

It can be noted here

(3.14) $$(grad\phi)^2 = \left(\frac{\partial\phi}{\partial x}\right)^2 + \left(\frac{\partial\phi}{\partial y}\right)^2$$

$$= \tau_{zy}^2 + \tau_{zx}^2$$

$$= \|\tau\|^2$$

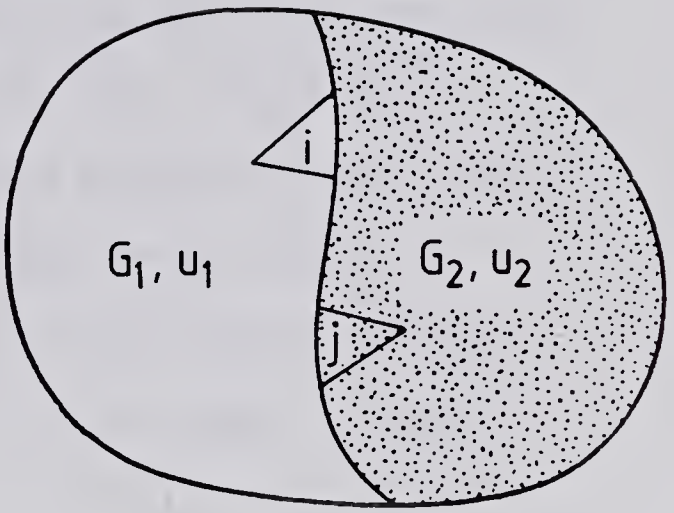

Fig. 3.1 Interchange of elements *i* and *j*

Hence the conclusion may be stated as:

> In order to improve the torsional rigidity of a certain nonhomogeneous bar, it is necessary and sufficient in the approximate sense to change the shear modulus distribution such that the higher stress area in the more flexible material region should be interchanged with the lower stress area in the stiffer material region.

3.2 Iterative Algorithm

To determine the maximum torsional rigidity, an iterative algorithm is constructed based on the conditions described previously as follows:

i) Select an initial shear modulus distribution such that it satisfies the constraint, eq.(2.19),

II) Compute the stresses in each element as well as the torsional rigidity of the cross-section,

iii) Select two elements; one of the highest stress from region *1*, the other of the lowest stress from region *2*,

iv) Define the new shear modulus function G_{r+1} which is locally different from G_r by interchanging the shear modulus in those two elements,

v) Repeat the steps ii), iii) and iv) until the maximum torsional rigidity is obtained.

The initial shear modulus function can be arbitrary as long as it satisfies the constraint. From then on the proportion of reinforcement will be kept the same by interchanging a pair of elements of the same area.

When the hybrid stress formulation is used in step ii) as in the case of the present study, the shear stresses in each element are calculated from the values of warping function instead of the Prandtl's stress function.

In step iii), the number of elements to be interchanged needs not be two, as several pairs of elements can be selected. In the present study, five pairs of elements were selected in the first step. This number was then reduced as the solution approached the optimum.

The interchange of the shear moduli of the elements in step iv) causes modification of the equations corresponding to the nodal points around these elements. This modified set of equations is then solved in step ii)

The iteration stops when either no element is chosen in step iii) or the interchange of even two elements results in a decrease of the torsional rigidity.

4. FINITE ELEMENT AND COMPUTER PROGRAM

4.1 Hybrid Stress Formulation

The hybrid stress approach suggested by Yamada et al.[22] is employed for the finite element torsion analysis in this study.

The cross-section of a prismatic bar is divided into a number of constant strain triangular elements, and these elements are classified into the 'inner' and 'boundary' elements. A boundary element is an element which possesses a side along the boundary of the cross-section. Figure 4.1 shows a typical element division and a boundary element.

The nodal points are numbered counter-clockwise *i-j-k* so that a boundary element should have *j* and *k* nodes on the boundary.

The stress function is assumed inside an element and is used for the stress boundary condition, while the warping function is defined along the three sides of an element so that the displacement is naturally continuous over the cross-section. Both the stress and warping are assumed linear in the Constant Strain Triangular elements (Figure 4.2).

In this case of hybrid stress approach, the relation between the stress and the warping function is then derived from the principle of minimum complementary energy. The complementary energy expression for a triangular element prism with unit thickness is

(4.1) $\Pi_c = U - W.$

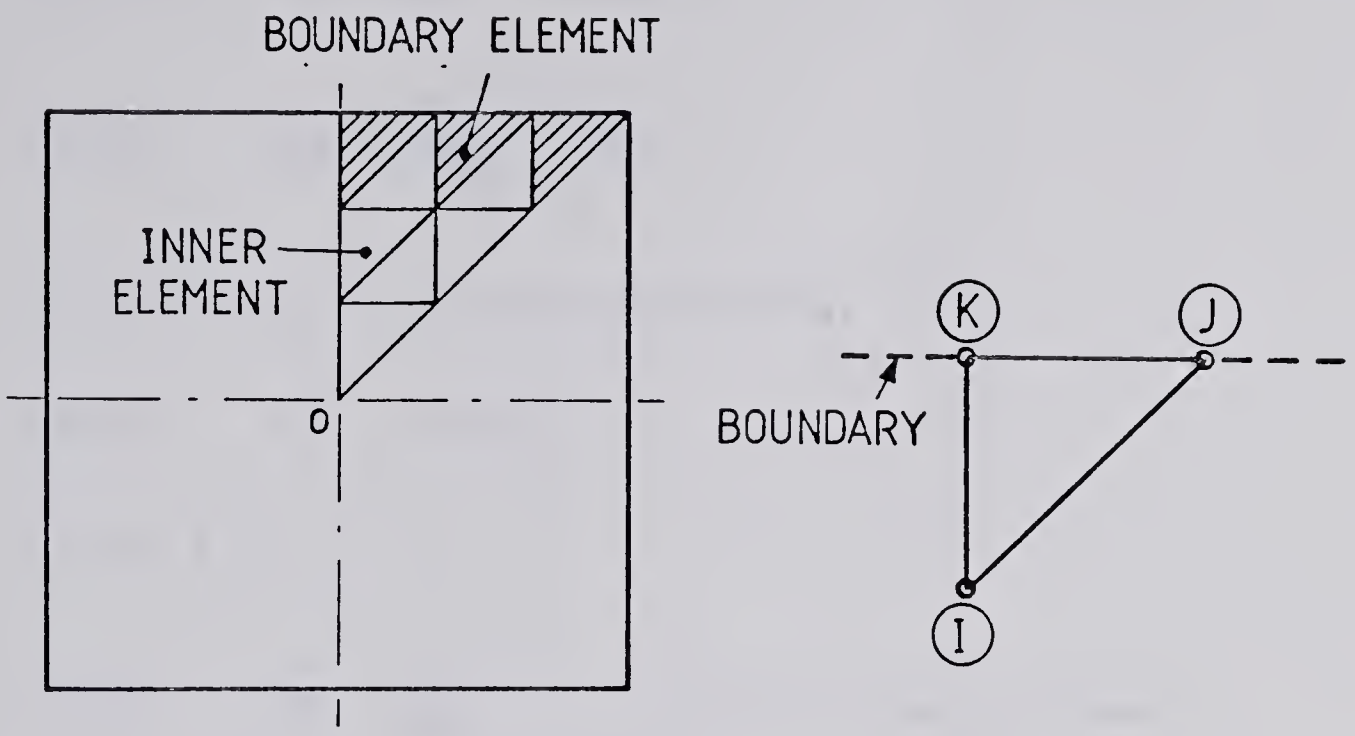

(a) Element classification (b) A boundary element

Fig. 4.1 'Inner' and 'Boundary' elements

The first term in the expression of the complementary energy, eq.(4.1) is the strain energy stored in an element prism with unit thickness

(4.2) $$U = \frac{1}{2}\iint_A \{\sigma\}^T [D] \{\sigma\} dxdy$$

where $\{\sigma\}$ is defined as

(4.3a) $$\{\sigma\} = \begin{Bmatrix} \tau_{zx} \\ \tau_{zy} \end{Bmatrix} = \frac{1}{2A} \begin{bmatrix} a_i & a_j \\ -b_i & -b_j \end{bmatrix} \begin{Bmatrix} \phi_i - \phi_k \\ \phi_j - \phi_k \end{Bmatrix}$$

for an inner element. Here in eq.(4.3a) A denotes the area

of the element and $a_i = x_k - x_j$, $b_i = y_j - y_k$ in cyclic order of i, j and k. For a boundary element with a side j-k along the boundary, $\phi_j = \phi_k = 0$ and eq.(4.3a) simplifies to

$$(4.3b) \qquad \{\sigma\} = \frac{1}{2A}\begin{Bmatrix} a_i \\ -b_i \end{Bmatrix}\phi_i ,$$

or in Pian's[17] original notation

$$(4.3c) \qquad \{\sigma\} = [P]\{\beta\}.$$

In eq.(4.3c),

$$(4.4a) \qquad [P] = \frac{1}{2A}\begin{bmatrix} a_i & a_j \\ -b_i & b_j \end{bmatrix} \text{ for an inner element,}$$

$$(4.4b) \qquad [P] = \frac{1}{2A}\begin{Bmatrix} a_i \\ -b_i \end{Bmatrix} \quad \text{for an for a boundary element}$$

and

$$(4.5a) \qquad \{\beta\} = \begin{Bmatrix} \phi_i - \phi_k \\ \phi_j - \phi_k \end{Bmatrix} \quad \text{for an inner element,}$$

$$(4.5b) \qquad \{\beta\} = \phi_i \qquad \text{for a boundary element.}$$

The matrix $[D]$ in eq.(4.2) denotes the inverse of the shear modulus

$$(4.6) \qquad [D] = \frac{1}{G}\begin{bmatrix} 1 & 0 \\ 0 & 1 \end{bmatrix} .$$

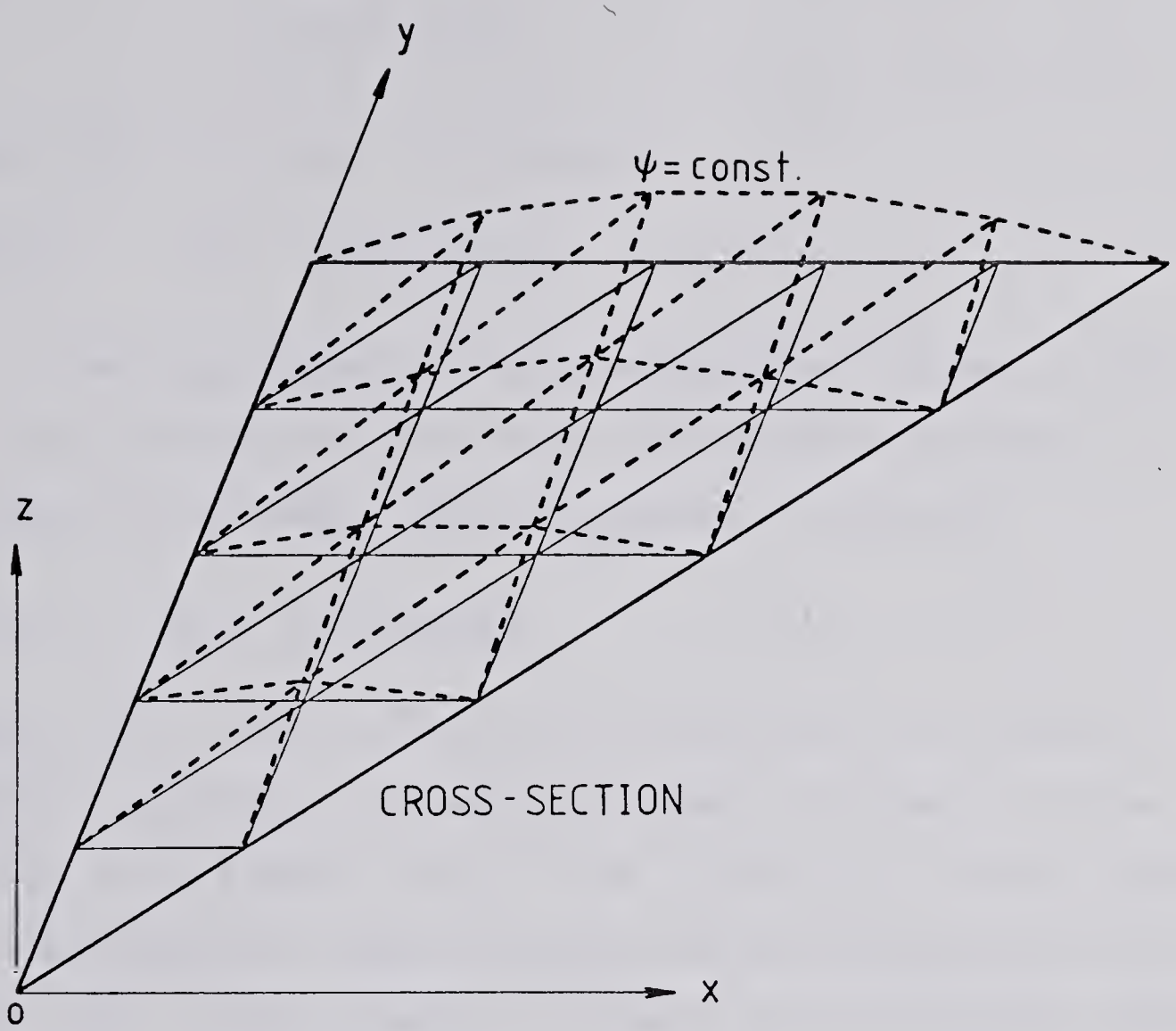

Fig. 4.2 Assumed warping function

If the integration in eq.(4.2) is carried out, the strain energy term becomes

$$(4.7) \qquad U = \frac{1}{2}\int\int_A \{\sigma\}^T [D] \{\sigma\} dxdy$$

$$= \frac{1}{2}\{\beta\}^T [H] \{\beta\},$$

where [H] is a matrix defined by

$$(4.8) \qquad [H] = A[P]^T [D][P].$$

The second part of the complementary energy is the work of the surface tractions over the boundary surfaces of an element prism where the displacement is defined

$$(4.9) \qquad W = \int_S \{T\}^T \{\psi_b\} ds$$

where $\{T\}^T = \langle M \;\; \tau_{jk} \; \tau_{ki} \; \tau_{ij} \rangle$ is the vector of twisting moment and normal components of shear stresses on three sides of an element; $\{\psi_b\}^T = \langle \theta \;\; \psi_{jk} \; \psi_{ki} \; \psi_{ij} \rangle$ is the vector of corresponding angle of twist and warping asssociated with the sides of the element. The work of the external loads W can now be integrated to

$$(4.10) \qquad W = \{\beta\}^T [P]^T [L] \{q_\psi\}.$$

Here,

$$(4.11) \qquad \{q_\psi\}^T = \langle \theta \;\; \psi_i \; \psi_j \; \psi_k \rangle$$

and

$$(4.12) \qquad [L] = \frac{1}{2}\begin{bmatrix} -2y_0 A & b_i & b_j & b_k \\ 2x_0 A & a_i & a_j & a_k \end{bmatrix}.$$

The complementary energy is then given from eqs.(4.1), (4.7) and (4.10) as

$$(4.13) \qquad \pi_c = \frac{1}{2}\{\beta\}^T [H]\{\beta\} - \{\beta\}^T [P]^T [L]\{q_\psi\}$$

Differentiating π_c with respect to $\{\beta\}$, and equating the result to zero, the realation is established as

$$(4.14) \qquad \{\beta\} = [H]^{-1} [P]^T [L]\{q_\psi\}.$$

The strain energy U can be expressed, by definition, in terms of stiffness matrix as

$$(4.15) \qquad U = \frac{1}{2}\{q_\psi\}^T [k]\{q_\psi\}$$

where $[k]$ is the stiffness matrix.

From the eqs.(4.7) and (4.14), and by noting that the martix $[H]$ is symmetric, the alternative expression for U can be derived as

$$(4.16) \qquad U = \frac{1}{2}\{\beta\}^T [H]\{\beta\}$$

$$= \frac{1}{2}\{q_\psi\}^T [L]^T [P][H]^{-1} [P]^T [L]\{q_\psi\}.$$

The element stiffness matrix associated with the hybrid approach is now obtained by equating the above two expressions, eqs.(4.15) and (4.16) for U as

$$(4.17a) \quad [k] = [L]^T [P][H]^{-1}[P]^T [L]$$

$$= \frac{G}{4A}\begin{bmatrix} 4A^2(x_0^2+y_0^2) & & & \text{Sym.} \\ 2A(a_i x_0 - b_i y_0) & a_i^2+b_i^2 & & \\ 2A(a_j x_0 - b_j y_0) & a_i a_j + b_i b_j & a_j^2+b_j^2 & \\ 2A(a_k x_0 - b_k y_0) & a_i a_k + b_i b_k & a_j a_k + b_j b_k & a_k^2+b_k^2 \end{bmatrix}$$

for the inner elements, and

$$(4.17b) \quad [k] = \frac{GA}{l_{jk}^2}\begin{bmatrix} (a_i y_0 + b_i x_0)^2 & & & \text{Sym.} \\ 0 & 0 & & \\ a_j y_0 + b_j x_0 & 0 & 1 & \\ -a_k y_0 - b_k x_0 & 0 & -1 & 1 \end{bmatrix}$$

for the boundary elements. Here, l_{jk}^2 denotes the squared length of the j-k side.

Furthermore, the stiffness matrix $[k]$, by its definition, connects the generalized force and displacement vectors as

$$(4.18a) \quad \begin{Bmatrix} M \\ F_i \\ F_j \\ F_k \end{Bmatrix} = [k] \begin{Bmatrix} 0 \\ \psi_i \\ \psi_j \\ \psi_k \end{Bmatrix}$$

or

$$(4.18b) \quad \{Q\} = [k]\{q_\psi\}$$

where F_i, F_j and F_k represent the resultant shear forces on the sides j-k, k-i and i-j, respectively. When the generalized force vectors of all the elements are assembled into the global vector, the scalar sum of these forces around a nodal point should be equated to zero so that the requirement of equilibrium may be fulfilled. In other words, eq.(4.18a) for the whole cross-section is assembled as

$$(4.19) \qquad \begin{bmatrix} k_{mm} & k_{mf} \\ k_{mf} & k_{ff} \end{bmatrix} \begin{Bmatrix} \theta \\ \psi_n \end{Bmatrix} = \begin{Bmatrix} M \\ F_n \end{Bmatrix}$$

The vector $\{F_n\}$ is a zero vector

$$(4.20) \qquad \{F_n\} = \{0\}, \quad n=1,2,3,..,\text{number of nodes.}$$

This means

$$(4.21) \qquad \{k_{mf}\}\theta + [k_{ff}]\{\psi_n\} = \{0\}$$

so that the torsional rigidity can be obtained as

$$(4.22) \qquad J = \frac{M}{G\theta l^4}$$

$$= k_{mm} - \{k_{mf}\}^T [k_{ff}]^{-1} \{k_{mf}\}$$

The stresses in each element can be calculated from

$$(4.23) \qquad \begin{Bmatrix} \tau_{zx} \\ \tau_{zy} \end{Bmatrix} = \frac{G}{2A} \begin{bmatrix} -2Ay_o & b_i & b_j & b_k \\ 2Ax_o & a_i & a_j & a_k \end{bmatrix} \begin{Bmatrix} \theta \\ \psi_i \\ \psi_j \\ \psi_k \end{Bmatrix}$$

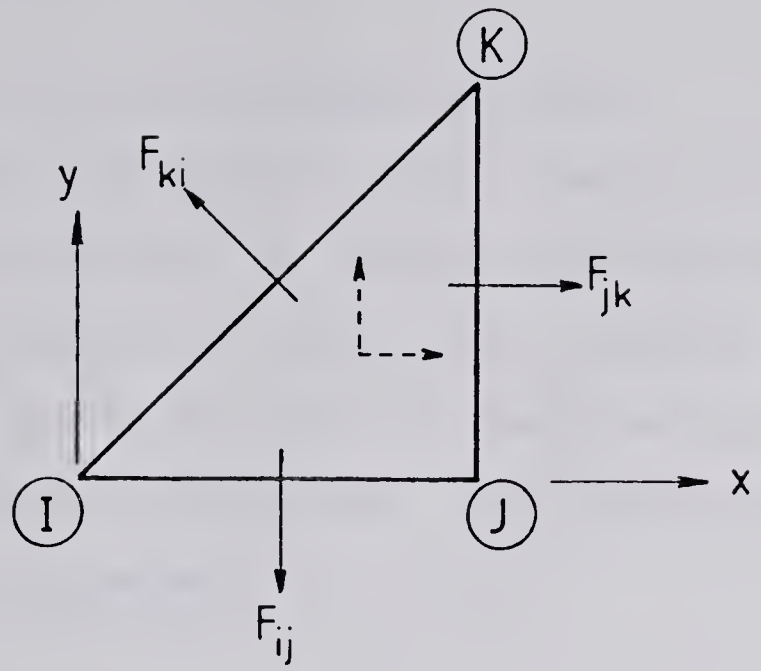

Fig. 4.3 Shear forces on the three sides of an element

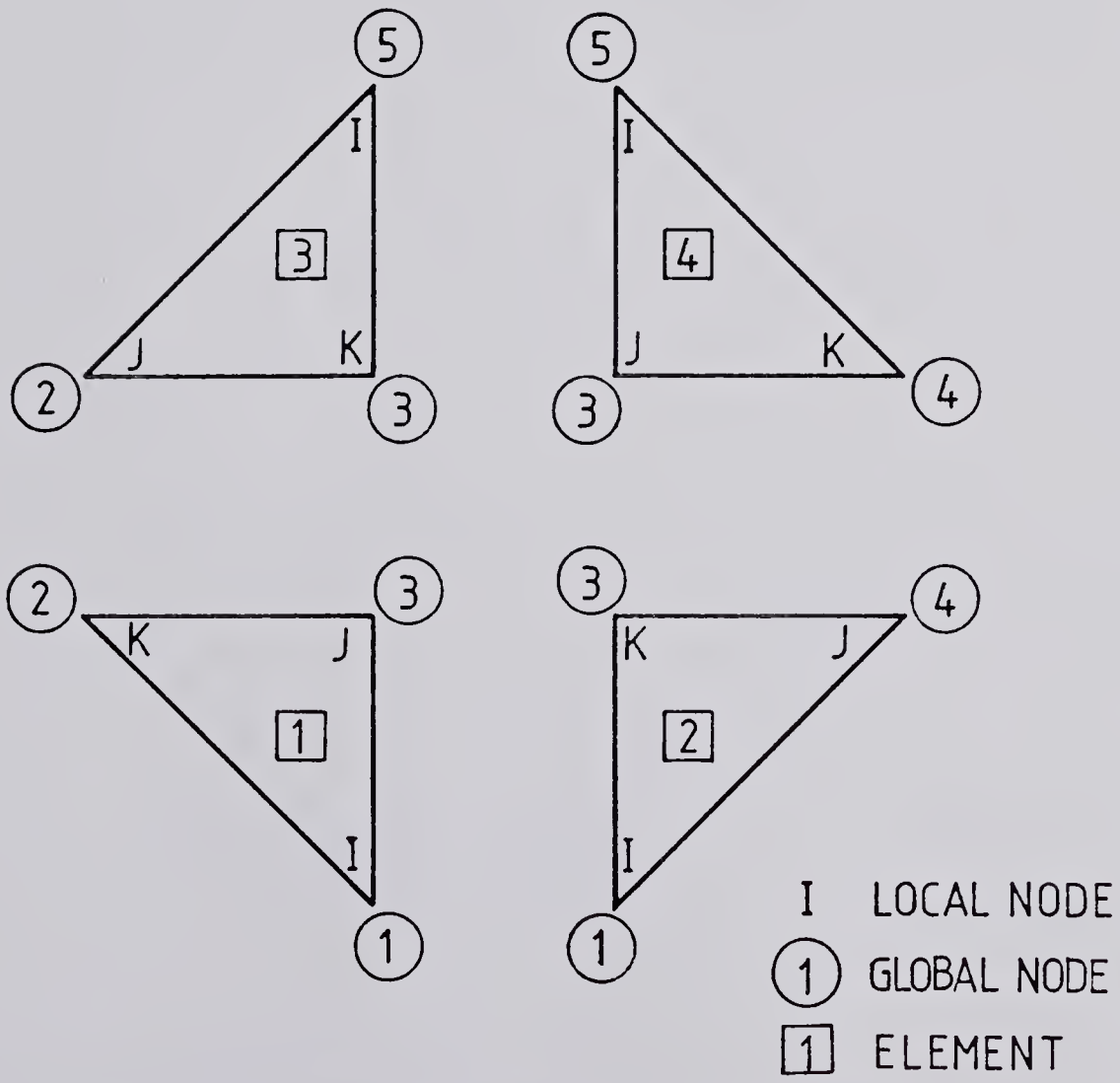

Fig. 4.4 Local and global numbering system of nodes and elements

4.2 Flow Charts of the Computer Program

The computer program for the present study of optimization is written in FORTRAN, and consists of MAIN and four major subroutines, namely; DATA, ASSEMB, SOLVE and STRESS. Flow charts for each of these subroutines are included in the next few pages. The complete program is attached in the appendix.

i) **MAIN** controls the sequence of computation by calling the subroutines, and makes the decision whether or not to carry out further iteration and if necessary, how many elements are to be interchanged.

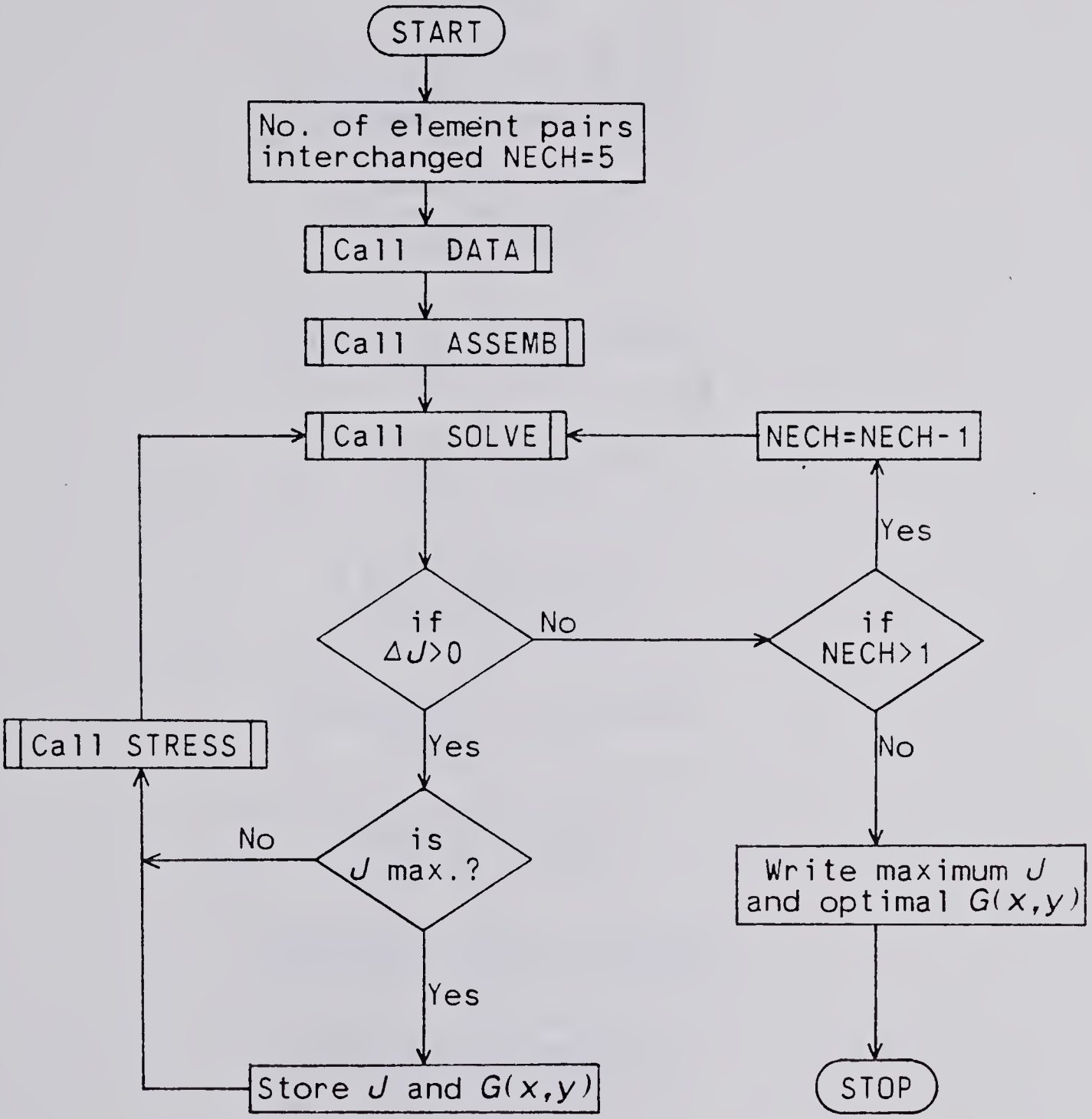

ii) Subroutine **DATA** reads the given nodal and element data, generates and completes the data for intermediate nodes and elements, prints out complete nodal and element data, and determines the number and band width of the equations to be solved.

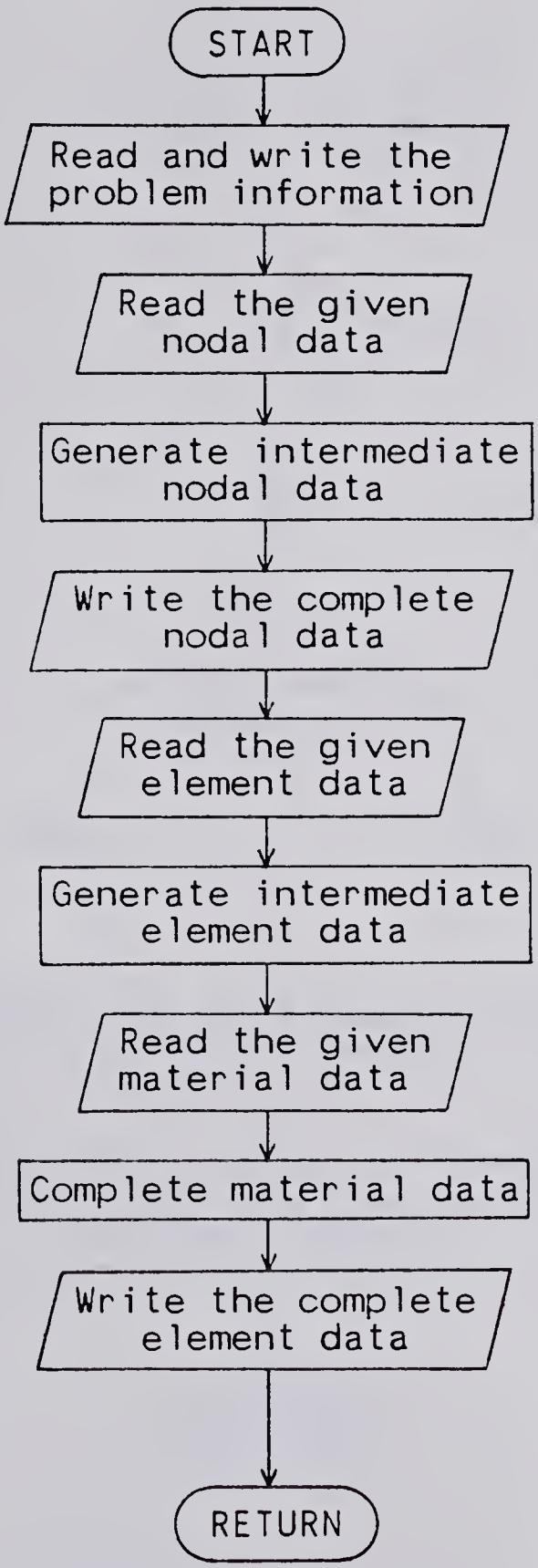

iii) Subroutine **ASSEMB** takes an element in turn, constructs an element stiffness matrix, assembles the global matrix and then applies the displacement boundary condition.

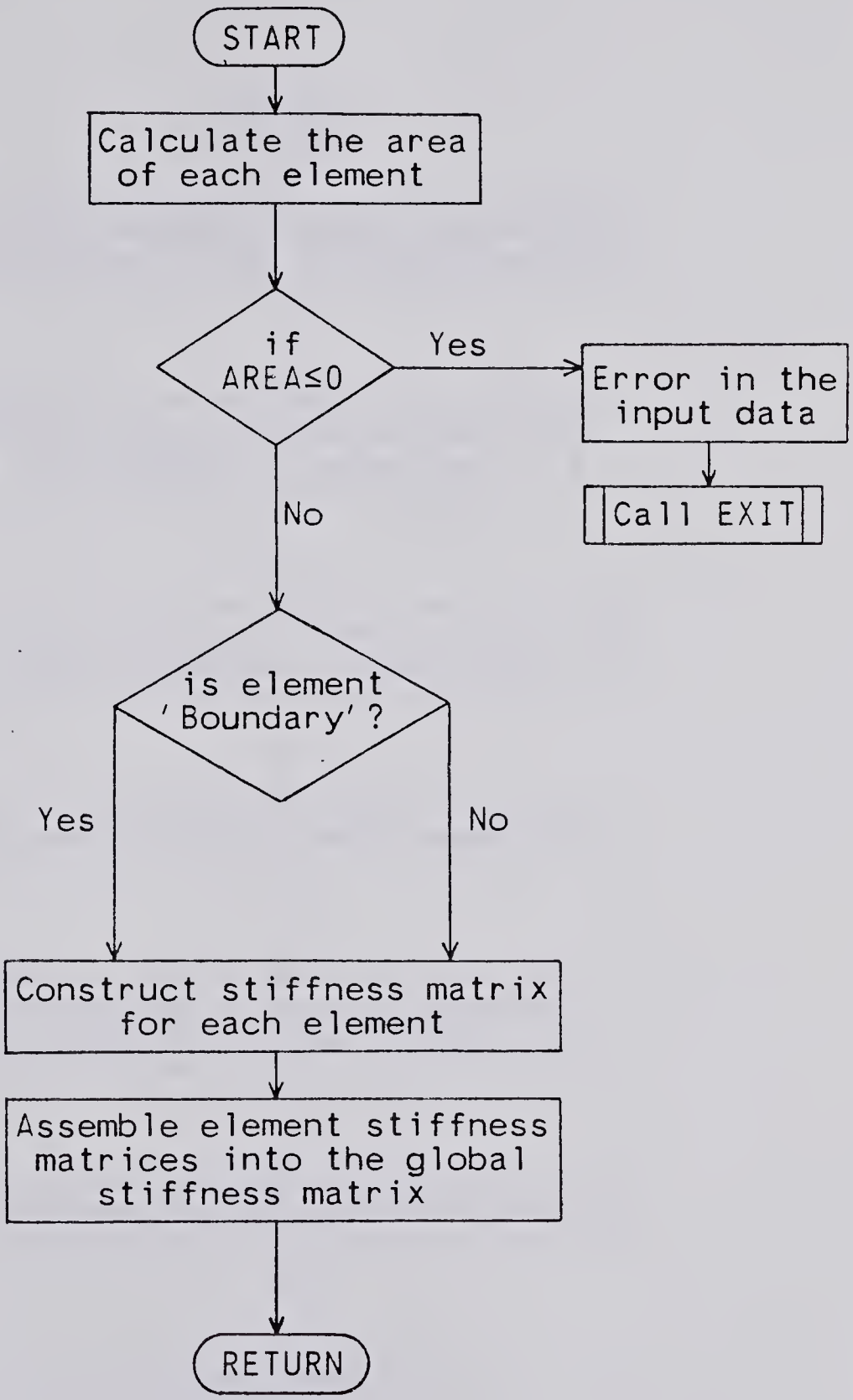

iv) Subroutine **SOLVE** solves eq.(4.23) for the values of warping function at the nodal points by using the Gaussian elimination technique then finds the torsional rigidity for the present shear modulus distribution.

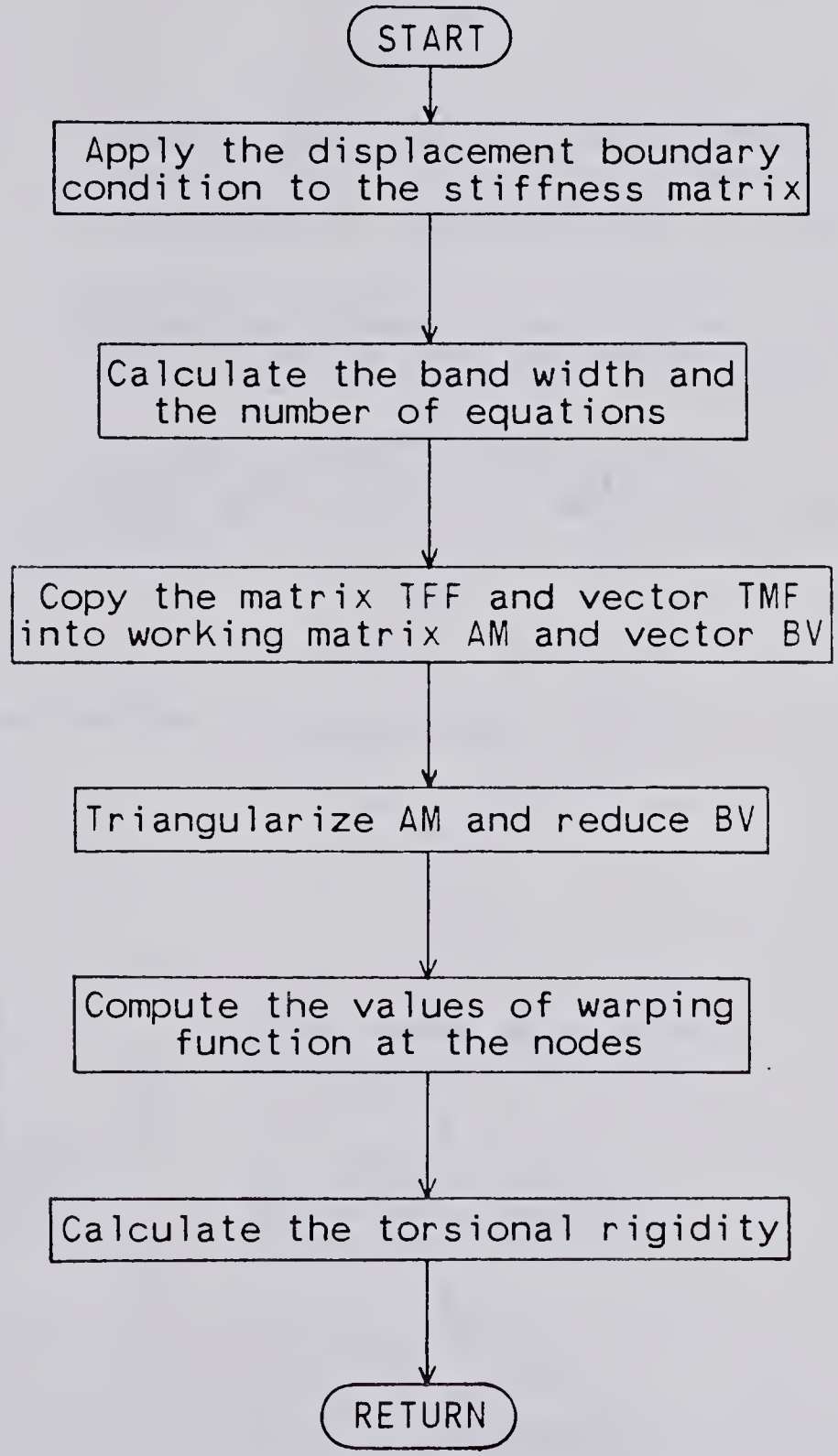

v) Subroutine STRESS calculates the shear stresses in each element, selects the elements to be interchanged, and modifies the stiffness matrix according to the new shear modulus distribution.

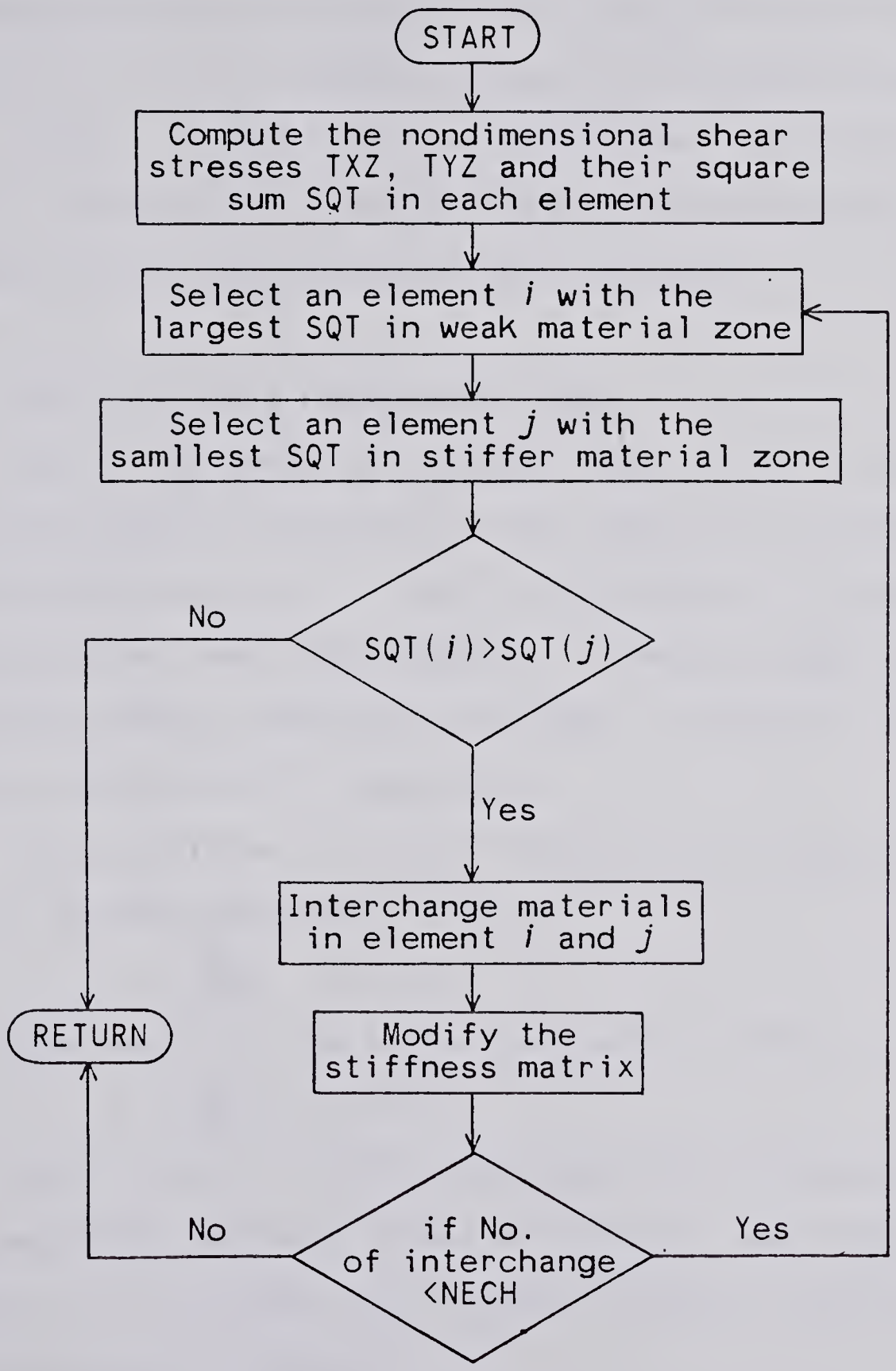

5. NUMERICAL TESTS AND RESULTS

5.1 Testing of the Numerical Procedure

As the solution procedure outlined in chapter 3 is not completely rigorous, it is necessary to demonstrate the uniqueness and convergence of the solution as well as the reliability of the computer program by considering special test cases. In the following subsections the results of the F.E.M. analysis for a bar with square cross-section are presented and compared with known solutions.

5.1.1 The case of a homogeneous bar

As a first numerical example, the finite element program based on the hybrid stress approach was applied to a homogeneous square bar. Due to the symmetry of the square cross-section, only one-eighth of it was divided into one hundred elements and sixty-six nodes. Figure 5.1 shows the element division of a square bar.

The calculated torsional rigidity for a square bar of side l in non-dimensional form is

$$J = \frac{M}{G\Theta l^4} = 0.1404$$

while the analytical solution is given in [20] as

$$J = \frac{M}{G\Theta l^4} = 0.1406$$

The torsional rigidity obtained with different numbers of element divisions is shown in Table 5.1 and Figure 5.3. Figure 5.3 also shows the torsional rigidity calculated by the displacement approach.

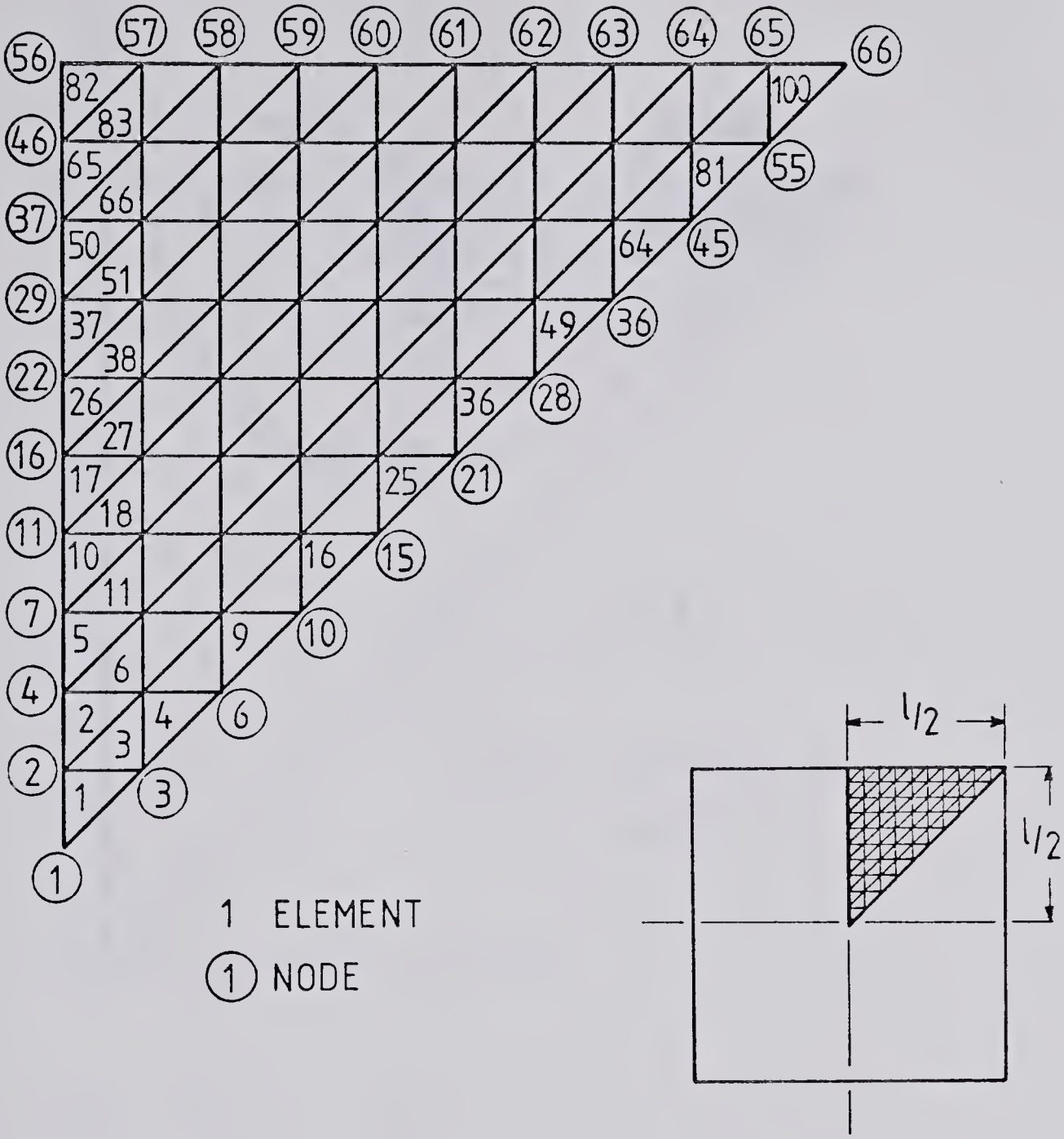

Fig. 5.1 Element division

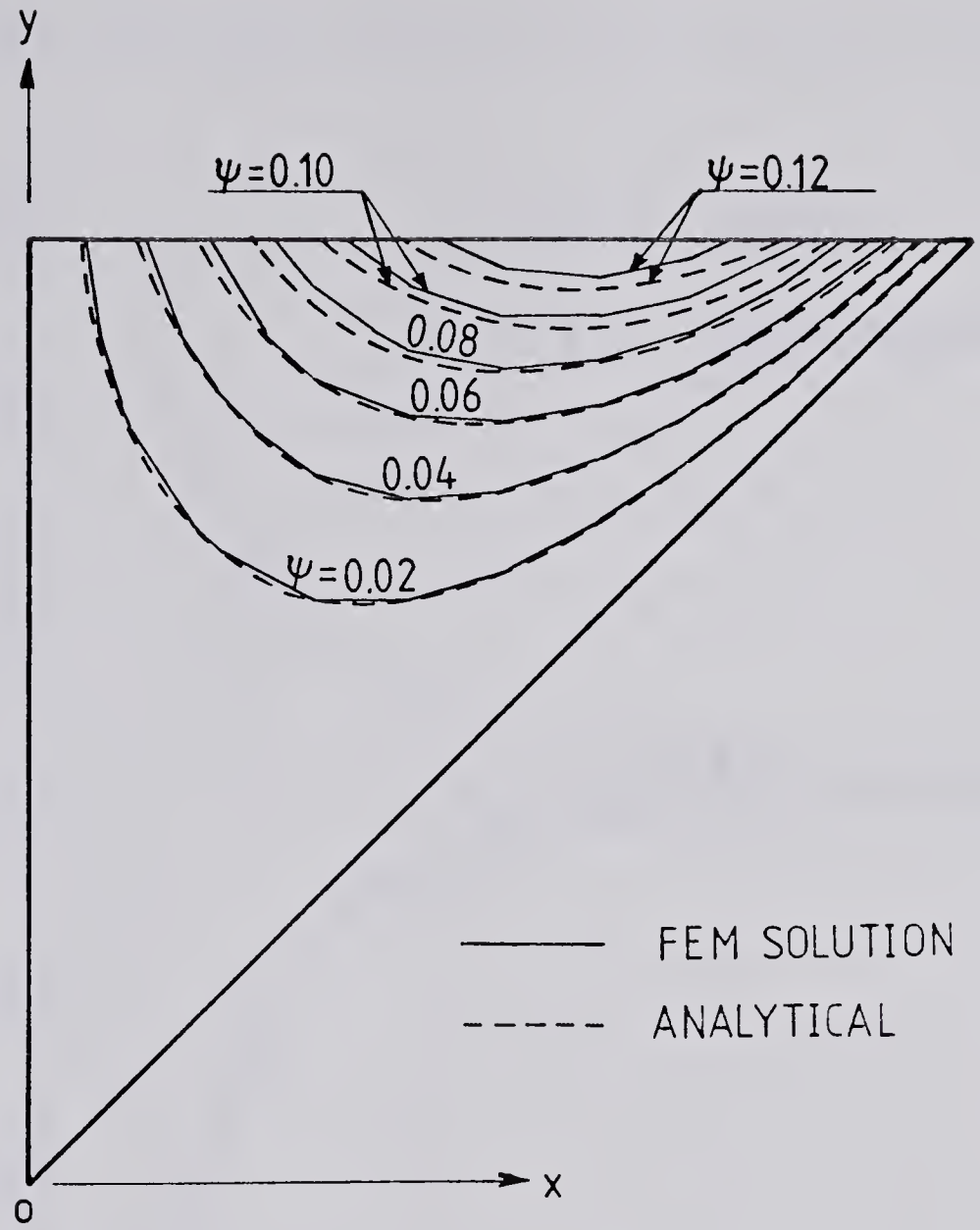

Fig. 5.2 Contours of constant warping on the cross-section of a homogeneous square bar

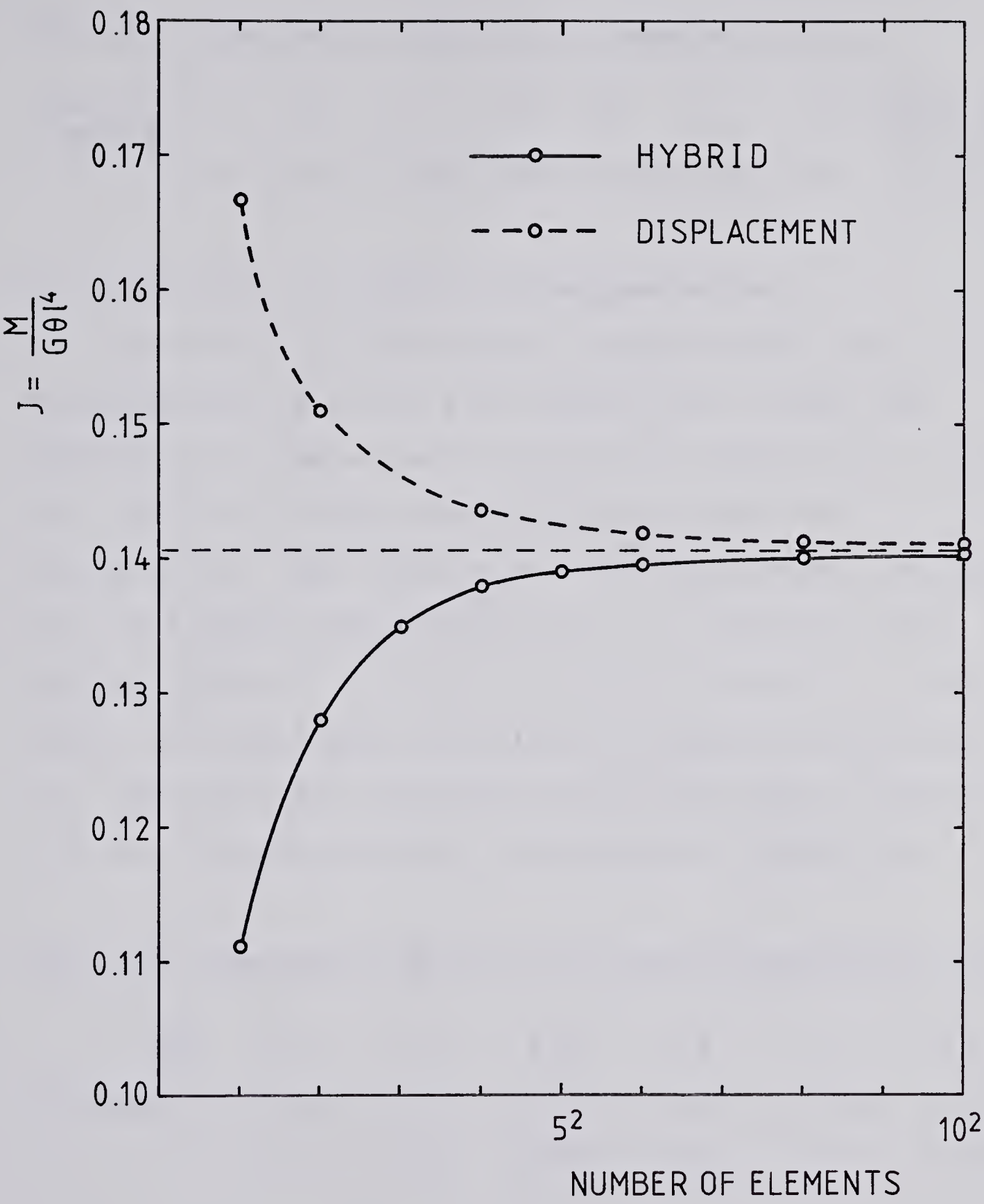

Fig. 5.3 Torsional rigidity of a homogeneous square bar

In addition, the contours of constant warping function are plotted in Figure 5.2.

Table 5.1 Torsional rigidity of a homogeneous bar

No. of elements	1^2	2^2	3^2	4^2	5^2	6^2	10^2	Analytical solution
J	0.111	0.128	0.135	0.138	0.139	0.140	0.140	0.141

5.1.2 The case of a simple nonhomogeneous bar

The results of the computer program in the case of nonhomogeneous bars were also checked for a square bar composed of two equal parts of different materials. In this case, one half of the square had to be taken into consideration - see Figure 5.4. The calculations were done with one hundred elements and sixty-six nodes and shear modulus ratios of 1.0, 1.5, 2.0, 3.0, 5.0 and 10.0. The results are tabulated and plotted in Table 5.2 and Figure 5.4. The analytical solutions calculated from a formula in [16] are also presented for the purpose of comparison.

Table 5.2 Torsional rigidity of a simple nonhomogeneous bar

$\frac{G_2}{G_1}$	1.0	1.5	2.0	3.0	5.0	10.0
FEM Result	0.139	0.170	0.195	0.236	0.306	0.458
	0.141	0.172	0.197	0.239	0.311	0.466

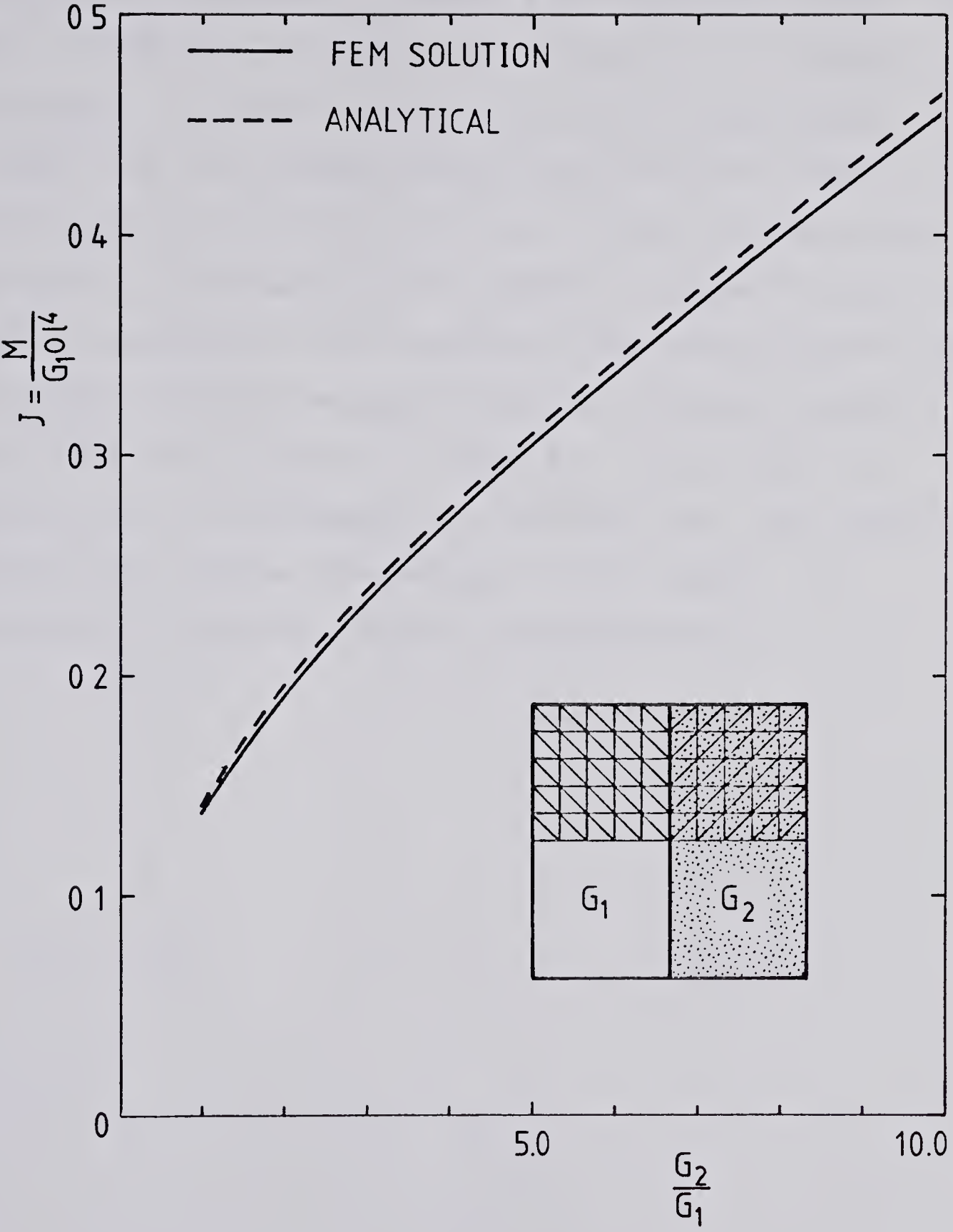

Fig. 5.4 Element division and the torsional rigidity of a simple nonhomogeneous square bar

5.1.3 The convergence and uniqueness

To test for the convergence to the optimal solution as well as its uniqueness, a square bar composed of 75% G and 25% G materials with shear modulus ratio of 1.5 was considered. An eighth of the cross-section was again divided into one hundred elements and sixty-six nodes. Starting from completely different initial distributions, the optimal distribution was computed. Figure 5.5 and 5.6 show the sequence of shear modulus distributions which were calculated in each iteration, and the torsional rigidity for each iteration is shown in Figure 5.7. Note that five elements were interchanged in the first step, the computer program then reduced this number by one whenever the increment of torsional rigidity became negative.

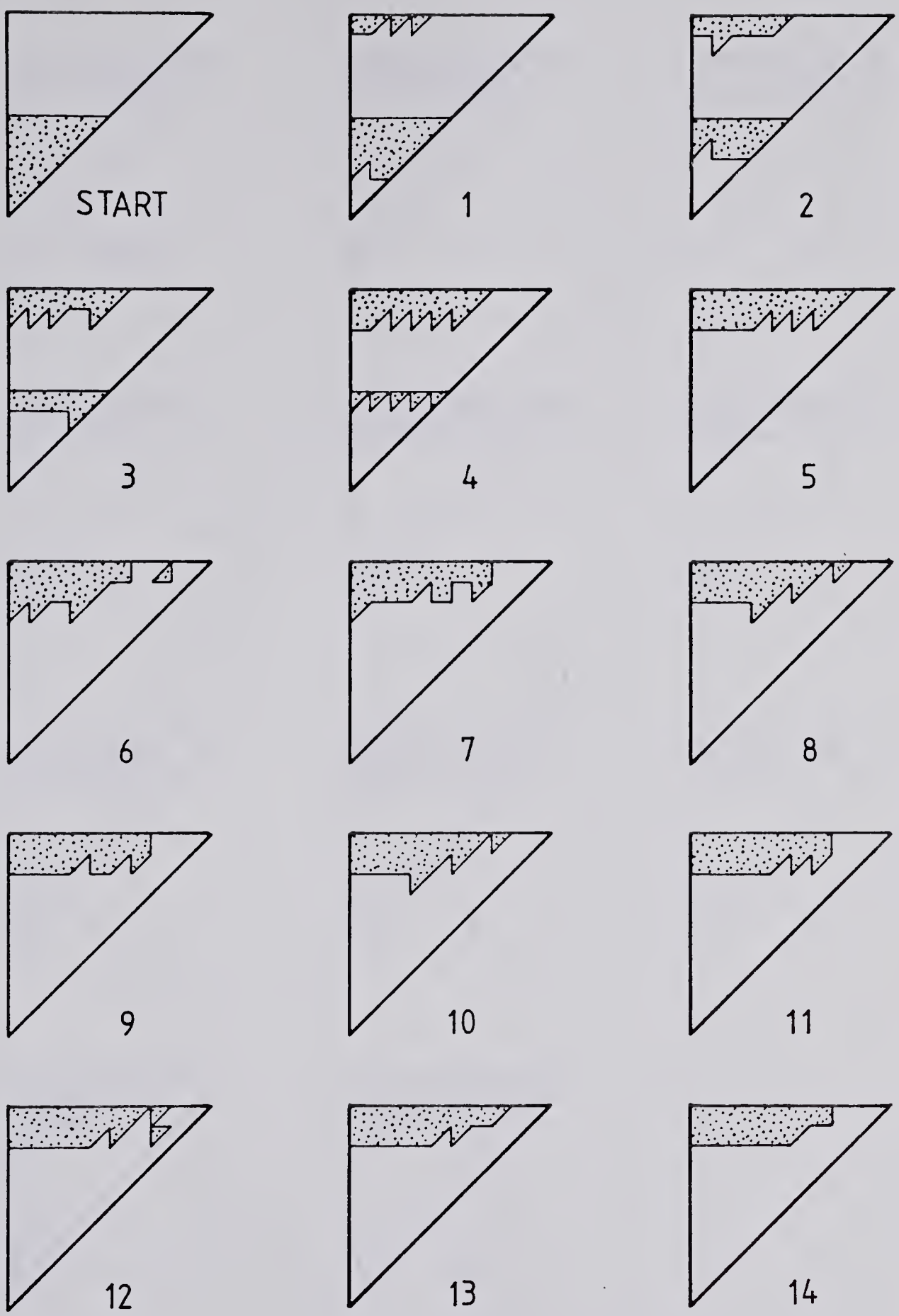

Fig. 5.5 Sequence of iteration starting with stiffer material in elements No.1-25

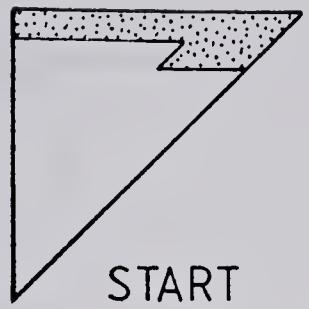

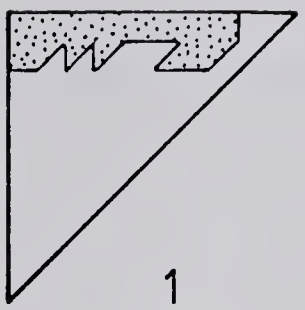

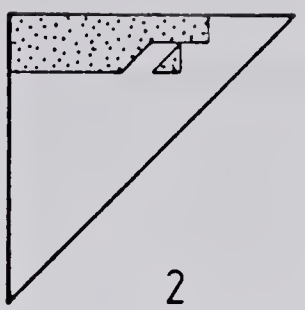

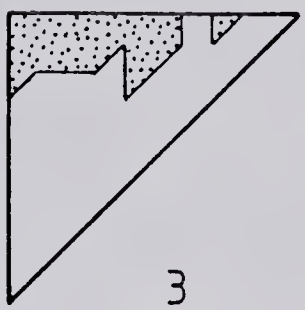

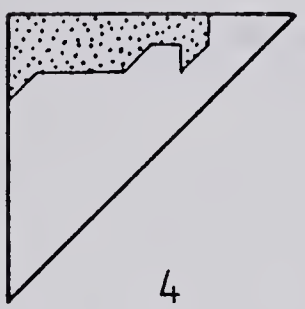

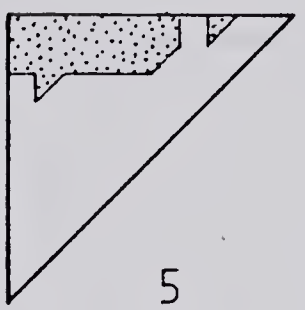

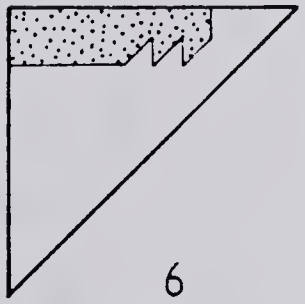

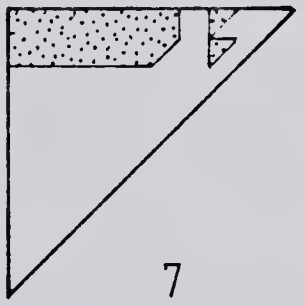

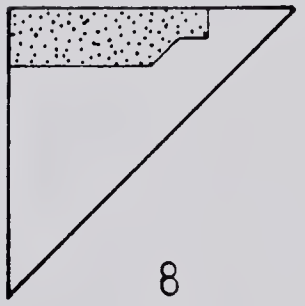

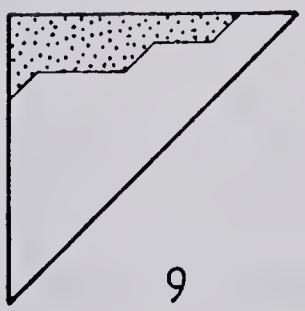

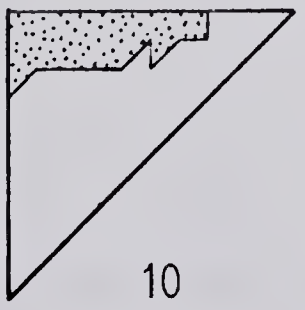

Fig. 5.6 Sequence of iteration starting with stiffer material in elements No.76-100

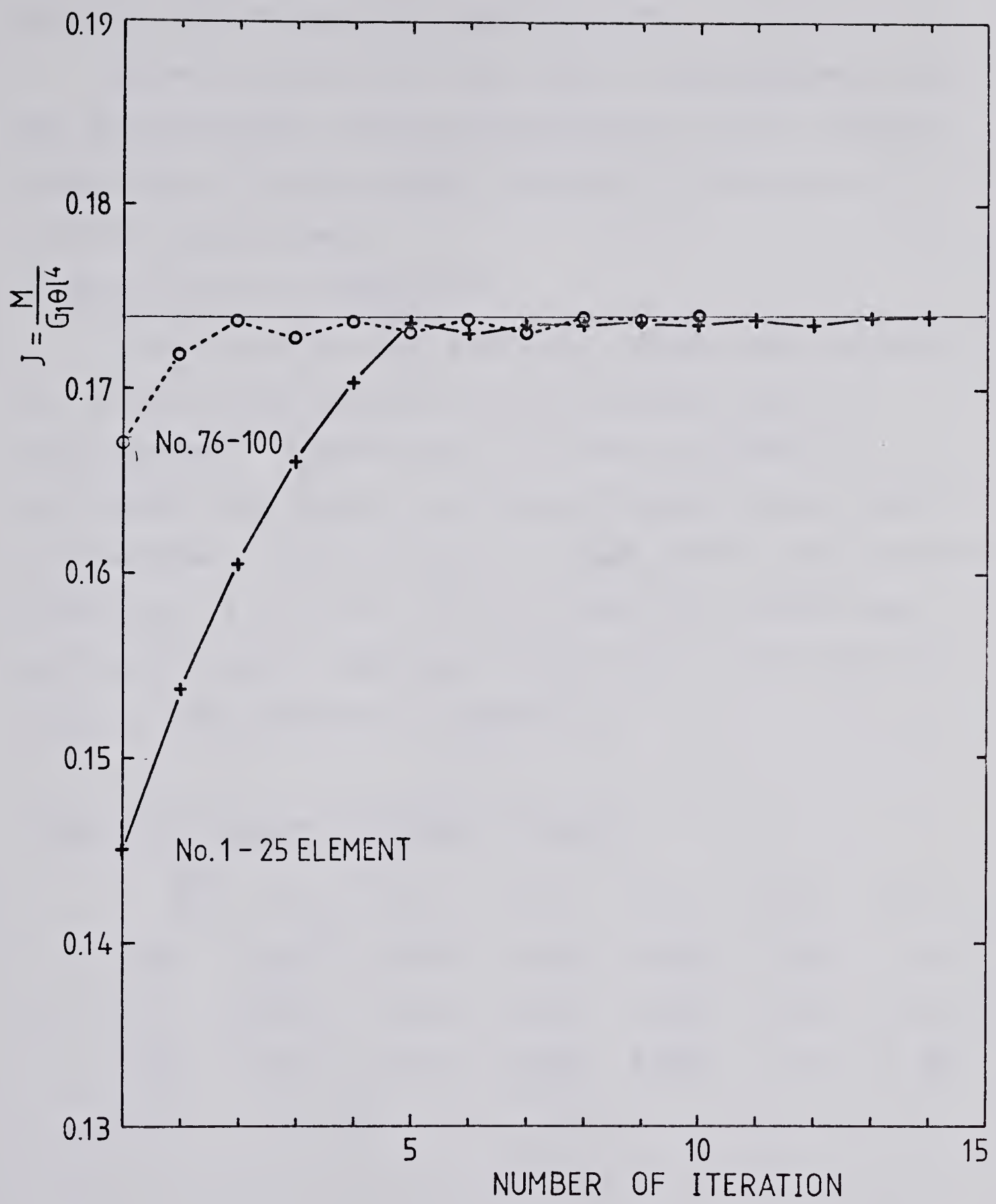

Fig. 5.7 Calculated torsional rigidity for different initial shear modulus distributions

5.2 Solutions for optimal nonhomogeneity

Optimal solutions for the square, nonhomogeneous bars are considered for various shear modulus ratios, and the comparisons of these optimal solutions to those of a circular bar are made.

i) Solutions for a square bar

A square bar of side *1* and unit length was considered for various shear modulus ratios and proportions of reinforcement. Figure 5.9(a), (b) and (c) show the optimizing distribution for three different proportions of reinforcement, 0.25, 0.5 and 0.75 each for the shear modulus ratios of 1.5, 2.0, 3.0, 5.0, 10.0 and 20.0 The maximum torsional rigidity obtained in each case is tabulated in Table 5.3 and plotted in Figure 5.8.

Table 5.3 Maximum torsional rigidity

	$\frac{G_2}{G_1}$	1.5	2.0	3.0	5.0	10.0	20.0
	0.25	0.174	0.205	0.265	0.386	0.683	1.238
p	0.5	0.193	0.245	0.348	0.556	1.072	2.102
	0.75	0.206	0.271	0.402	0.663	1.316	2.621

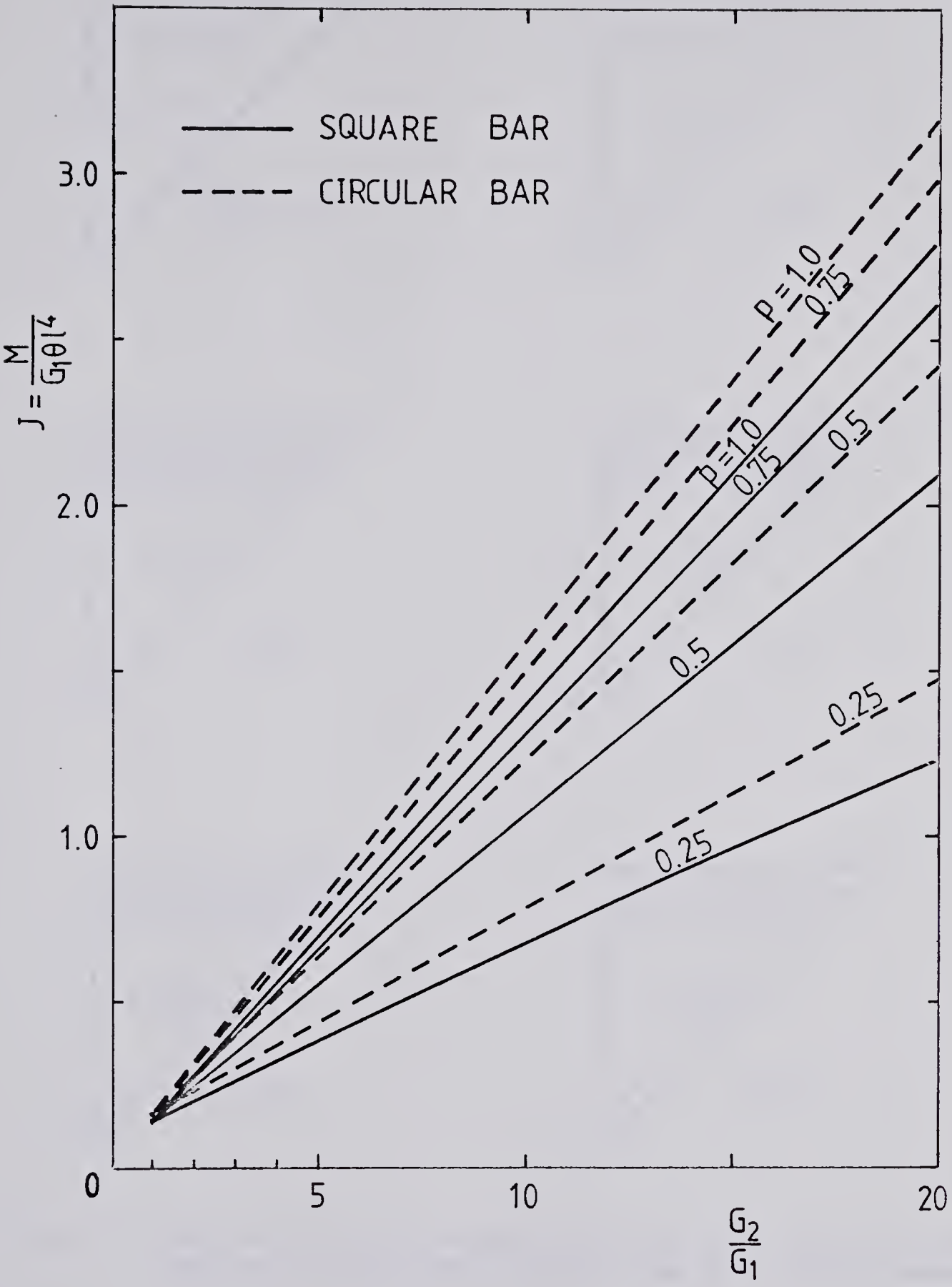

Fig. 5.8 Optimal nonhomogeneity of a square bar

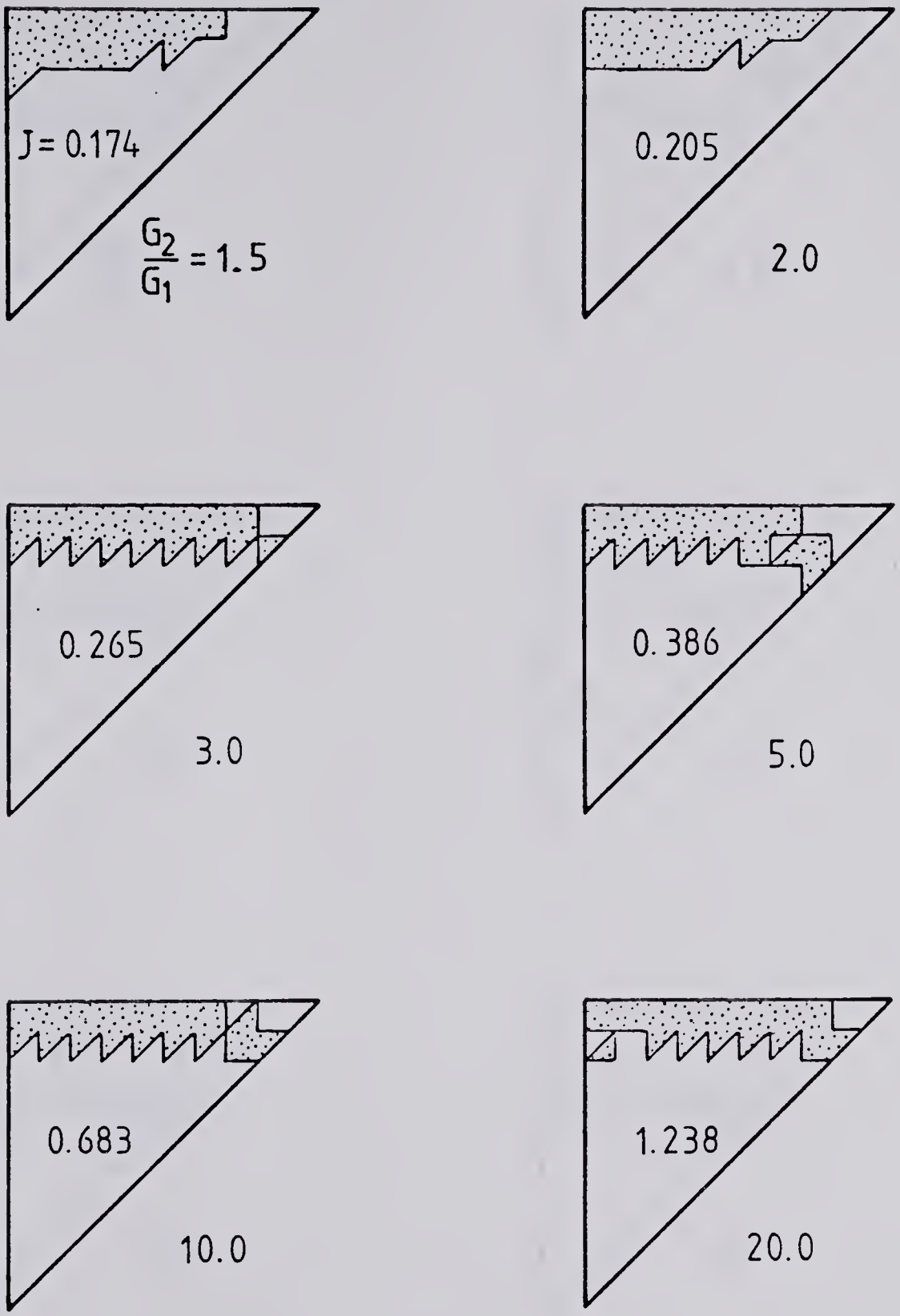

Fig. 5.9 The maximum torsional rigidity for various shear modulus ratios and proportions of reinforcement

(a) p = 0.25

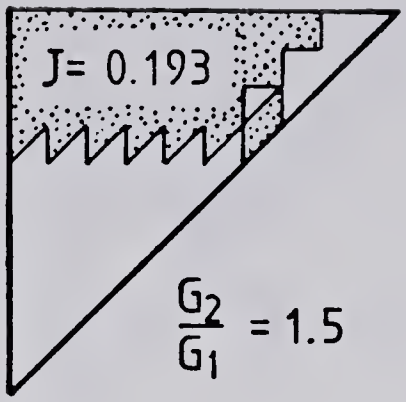

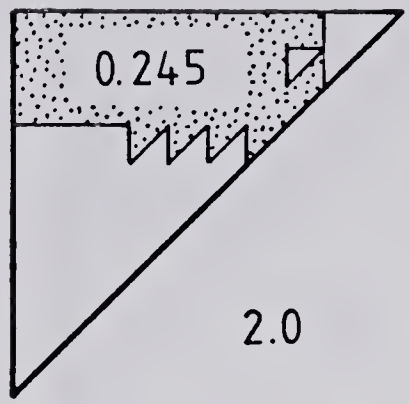

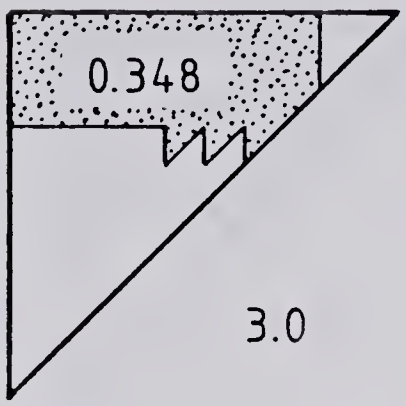

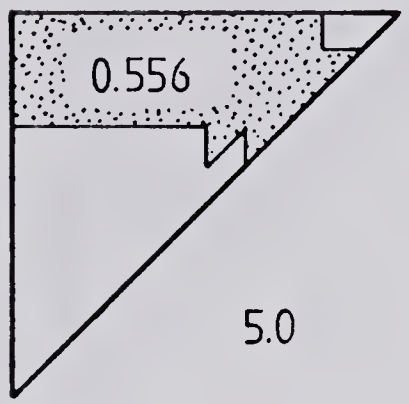

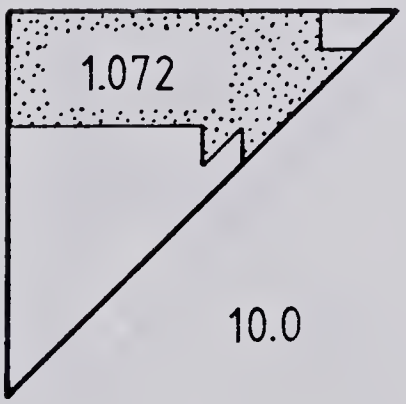

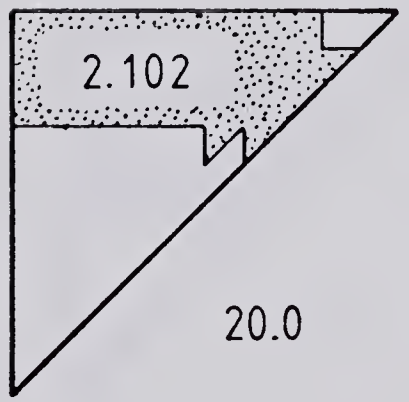

(b) p = 0.5

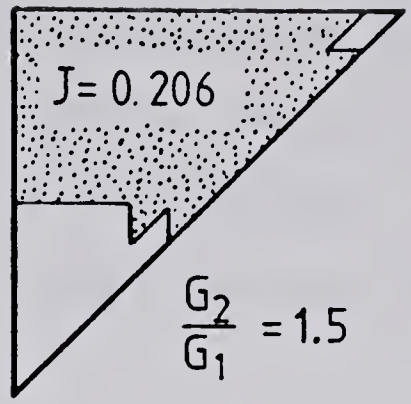

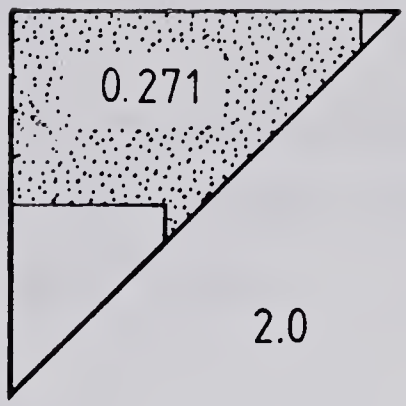

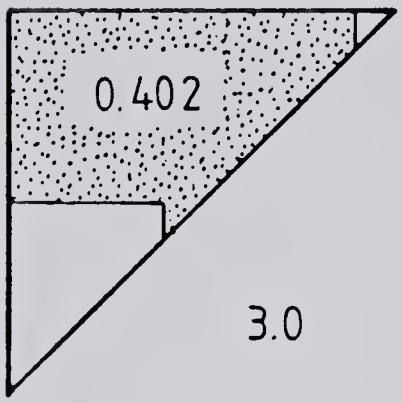

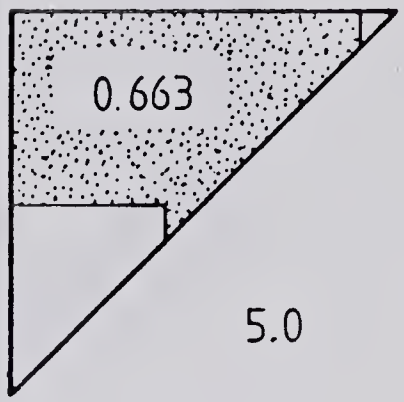

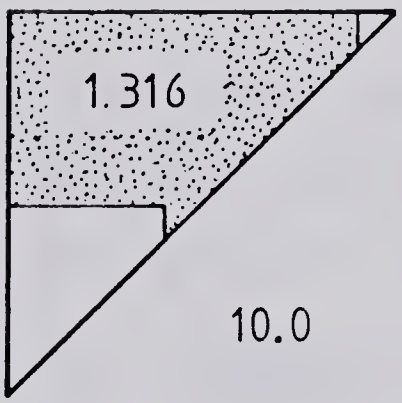

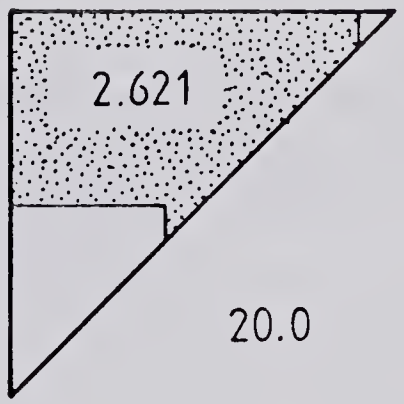

(c) $p = 0.75$

5.3 Optimal Solutions of a Circular Bar

To compare the optimal solution of the square bar with that of a circular bar, a circular bar with radius *a* which has the same cross-sectional area is considered.

Since

$$(5.1) \qquad \pi a^2 = l^2$$

then

$$(5.2) \qquad a = \frac{l}{\sqrt{\pi}}.$$

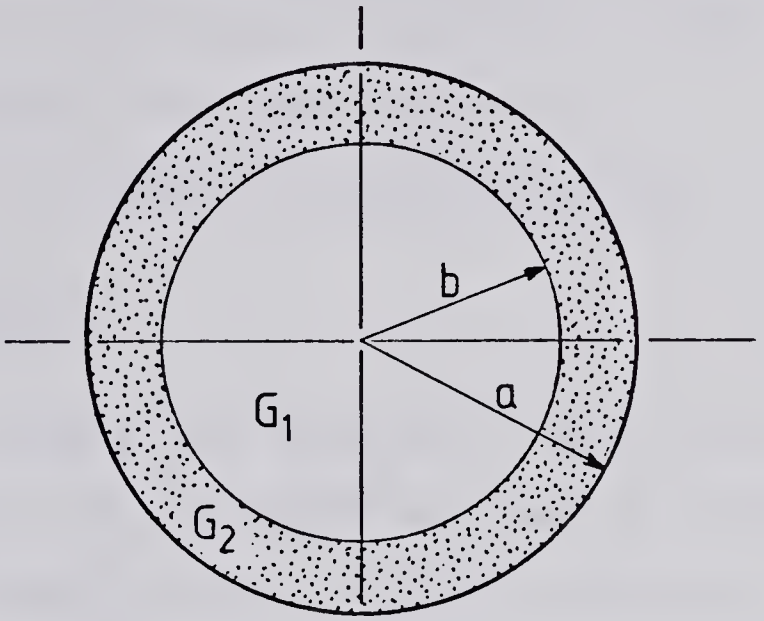

Fig. 5.10 Optimum nonhomogeneous circular bar

It can be easily shown that the optimal nonhomogeneous circular bar is of the form as illustrated in Figure 5.10, of which the torsional rigidity is given as

$$(5.3) \qquad J_{op} = \frac{\pi}{2}\left(\frac{G_2}{G_1}(a^4-b^4) + b^4\right).$$

The proportion of reinforcement is simply the ratio of the ring area to that of entire cross-section

$$(5.4) \qquad p = 1-\frac{b^2}{a^2} \ .$$

The substitution of eq.(5.4) into eq.(5.3) gives the expression of the maximum torsional rigidity in terms of p as

$$(5.5) \qquad J = \frac{\pi a^4}{2}\left[\frac{G_2}{G_1}\{1-(1-p)^2\} + (1-p)^2\right].$$

For a fixed shear modulus ratio, the optimal torsional rigidity is a quadratic function of p and is a linear function of shear modulus ratio for a given p.

Now define the efficiency of optimization as

$$(5.6) \qquad eff. = \frac{J_{op}-J_1}{p(J_2-J_1)}$$

where J , J and J denote the torsional rigidities of homogeneous bars made of G_1, G_2 materials and of optimal nonhomogeneous bar, respectively. This efficiency of optimization can be understood as the ratio of the improvement in the torsional rigidity to the expected improvement with the same amount of stiffer material if the increment of the torsional rigidity were proportional to the amounts of stiffer material being reinforced. From the eqs.(5.3), (5.5) and (5.6), the expression of the efficiency of optimization can be derived in terms of p for a circular bar as

$$(5.7) \qquad eff. = 2-p.$$

These efficiencies for a circular and a square bar depending on the proportion of reinforcement can be seen in Figure 5.11.

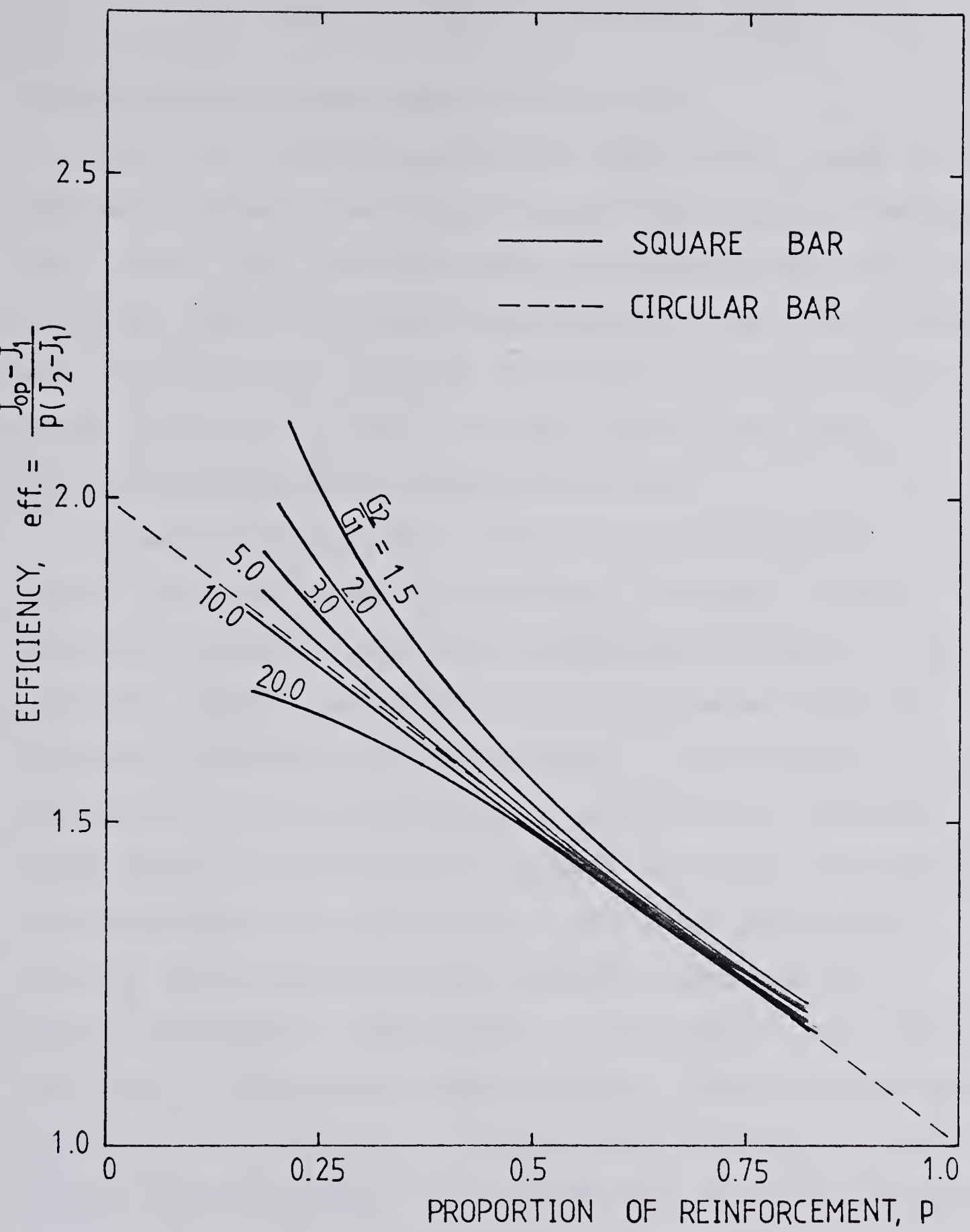

Fig. 5.11 Efficiency of optimization

1. DISCUSSION AND CONCLUDING REMARKS

1.1 Discussion of the Solution Procedure

The F.E.M. solution procedure used in this study is a compromise between the using a very simple element combined with a trial and error procedure for optimization, and that of using a complex element combined with a very fine element mesh. The simplest approach may be too crude to find an answer close to the actual optimum, while the latter approach would be quite expensive to use.

As seen in Figure 5.3, the calculated torsional rigidity for a homogeneous square bar converges to the analytical solution with increasing element numbers. The torsional rigidity obtained by the displacement approach instead of the hybrid stress approach is also shown in Figure 5.3. It is interesting to note that the torsonal rigidity by the displacement approach converges from above the known solution (upper bound), while the torsional rigidity by the hybrid stress approach converges more rapidly from below (lower bound). Furthermore, the stress solutions by the hybrid stress approach should also be more accurate than those by the displacement approach. Since the stress in each element is to be compared in order to select a pair of elements for interchange, the hybrid stress approach was employed in the present study. A more detailed discussion of the use of displacement and hybrid stress approach can be found in [3,22].

In the actual computer program, the shear stresses are nondimensionalized and then compared, i.e., the the shear stress divided by the shear modulus is used for selecting elements to be interchanged. This is mainly for the reason that the elements in the stiffer material region can always have higher stresses when the shear modulus ratio is high enough so that the interchange of the shear modulus distribution can not be accomplished. Also by interchanging more elements, more shear modulus distributions may be considered with the result that the chance of missing the best one may be reduced.

Five pairs of elements at the most are to be chosen in the first iteration and this number is reduced by one whenever the increment of torsional rigidity becomes negative. This number can be arbitrarily set, in fact, one may choose any number of element pairs to begin. However, if too many elements are interchanged, the assumption that the change of stresss function is small may be violated; if too few, it may cause extremely small changes in the torsional rigidity.

The size of element in the present study was taken as constant for all elements. However, the computer program can be modified so that it can take different size elements. It would be possible therefore to improve the accuracy of solutions by having a finer element mesh in the higher stress region around the center of the lateral surface of the bar.

6.2 Discussion of Results

The test results of a homogeneous square bar show the error of the calculated torsional rigidity by the hybrid stress approach being 1.2% and 0.2% with 25 and 100 element divisions, respectively (Table 5.1 and Figure 5.2), while the errors for the nonhomogeneous bar vary from 1.2% to 1.7% depending on the shear modulus ratio (Table 5.2 and Figure 5.4). Although half of the square instead of an eighth section is taken and divided into 100 elements in the case of a simple nonhomogeneous bar, the size of the element is same as for an eighth of a homogeneous square with 25 elements. It is therefore expected that the errors should be similar in these two cases in the range of low shear modulus ratios. The error increases as the difference of material constants increases. This means that the results in this study are more reliable for lower shear modulus ratios.

Figure 5.5 and 5.6 show that the optimal solution is essentially unique regardless of initial shear modulus distribution, and that the sequence of G or u converges to this solution. The final solution in Figure 5.5 and 5.6 appear to be different, however the difference in torsional rigidity is very small (less than 0.005%). The true optimal solution must be near these two shapes and any solutions close to these two may be considered optimal for practical purposes.

The approximate uniqueness of solution can be shown for the shear modulus ratios other than 1.5, as well. However, as the shear modulus ratio increases, not only does the accuracy of the solution decrease but also it requires more iteration steps. Eventually, it becomes almost impossible to arrive near the optimal solution when the given initial shear modulus distribution is too far from the final solution. For this reason the example given is presented for a shear modulus ratio of 1.5.

Figure 5.9 illustrates the obtained maximum torsional rigidity depending on the proportion of reinforcement as well as on the shear modulus ratio. The maximum torsional rigidity in the case of a circular bar is linearly proportional to the shear modulus ratio as shown in the eq.(5.7). In the case of a square bar, the trend is almost the same,i.e., linearly dependent on the shear modulus ratio, except for p=0.25. It is also seen from Figure 5.11 that the maximum torsional rigidity for the high shear modulus ratio and low proportion of reinforcement is less than anticipated thus the efficiency of optimization of a square bar falls below that of a circular bar. This is mostly due to the crude shape of the material boundaries when approximated by the element triangles. As seen in Figure 5.8(a) the shape of the rigid reinforcement of the optimal solution is quite smooth in the lower shear modulus ratio (1.5, 2.0) range, but it becomes very rough in the higher shear modulus ratio range.

In order to investigate this effect, the optimal shear modulus distribution for p=0.25 and shear modulus ratio 10.0 was considered. Since the F.E.M. solution is only an approximate representation of the optimal shear modulus ratio, the actual shape of the optimal rigid reinforcement should be bounded by a smoooth curve close to the saw-tooth shape. If the solution represented by the solid lines in Figure 6.1 is considered, the torsional rigidity is found to be

$$J = 0.696$$

which is almost 2% higher than the previously obtained value of 0.683. The efficiency of optimization can then be calculated to be

$$eff. = 1.754$$

which would bring the curve of shear modulus ratio 10.0 in Figure 5.11 just above the dotted straight line for a circular bar.

As is clear from the above discussion, the results of optimal solutions presented in Chapter 5 are approximate and thus can be used only for a qualitative study of the behaviour of such optimal solutions.

The optimal shear modulus distribution obtained for the different shear modulus ratios and proportion of reinforcement are illustrated in Figure 5.9(a), (b) and (c). One may notice that the zones of rigid reinforcement for lower shear modulus ratios and lower proportions of reinforcement start to build up around the center of lateral

surface then with increasing amounts of stiffer material, the zones expand to form a belt shape around the center of the cross-section. This observation is quite consistent with the conclusions found in [10] and [14], although the shear modulus or the yield limit in their study is a continuous function, not like the shear modulus function in this study.

The efficiency of optimization for a circular bar is represented as a straight line in Figure 5.11. It is very interesting that the efficiency of optimization for a square bar is much higher than that of a circular bar especially in the range of low shear modulus ratio and low proportion of reinforcement. It is no wonder that the former approaches to latter with the increasing shear modulus ratio and proportion of reinforcement, because the zones of stiffer material in the optimal solutions for a square bar resemble the ring shape like the case of a circular bar in the high shear modulus ratio and proportion of reinforcement range as previously discussed.

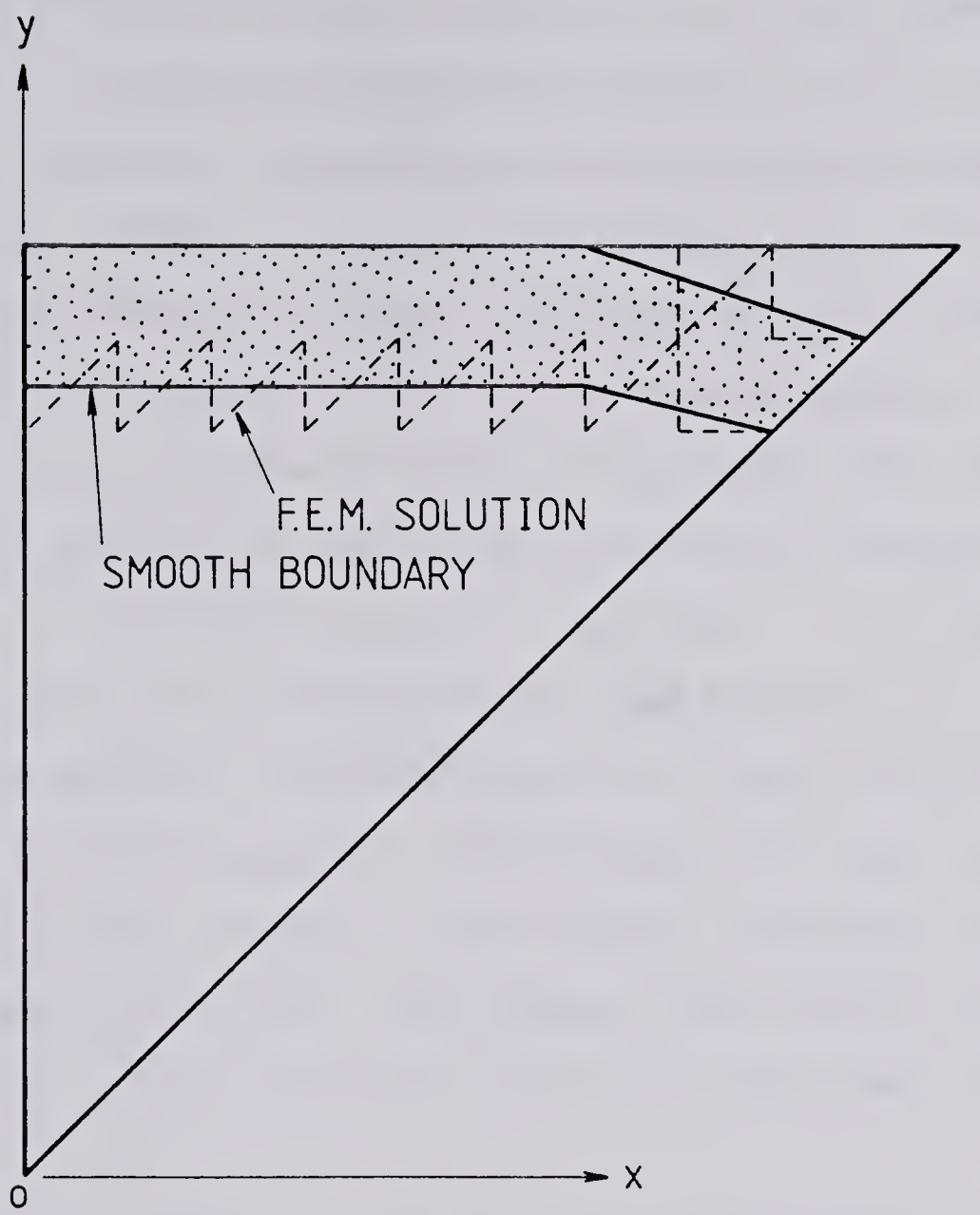

Fig. 6.1 Boundaries of the zones of optimal rigid reinforcement are made smooth

6.3 Concluding Remarks

The study of optimal nonhomogeneity by Klosowicz[9,10] for elastic torsion and by Mioduchowski [13,14] for plastic torsion revealed interesting characteristics of such optimal solutions. Zones of rigid reinforcement start to appear around the center of lateral surfaces where the shear stress would be the highest if the bar were homogeneous, then the configuration changes to form a ring around the center of the cross-section as the ratio of material constants or the amount of the stiffer material increases. It is more likely that the practical problem often encountered is of the type where the material constants vary in a jump like manner rather than continuously. Even though the shear modulus function in this study is restricted to assume either of two shear moduli G_1 or G_2 , the optimal distribution for a square bar behaves similarly and hence the same conclusion is drawn.

Another aspect of the optimal solution was also noted in the comparison of square and round cross-sections. It was shown that a square bar subjected to torsion can be more efficiently optimized; than a circular bar; more improvenent in torsional rigidity with a smaller amount of stiffer material.

Although only bars with square cross-section were considered in the present study, it could be extended to the bars with cross-section such as an ellipse or triangles, by

using essentially the same computer program. In addition, different sized elements could be easily included in the procedure.

It is further believed that the method used and the solution procedure followed in the present study can be applied to the similar optimization problems in other fields such as ground water seepage or heat transfer.

REFERENCES

1. Banichuk, N. V., "Optimization of elastic bars in torsion", Int. J. Solids Struct., Vol.12, pp 275-286(1976)

2. Cea, J. and Malanowski, K., "An example of a max-min problem in partial differential equations", SIAM J. of Control, Vol.8, No.3, pp 305-316(1970)

3. Desai, C. S.,*Elementary Finite Element Method*, Prentice Hall, N.J.(1979)

4. Feldmann, J. M., "Direct numerical determination of stresses in elastic solids as illustrated by the torsion problem", Int. J. Solids Struct. Vol.4, pp 675-688(1968)

5. Herakovich, C. T. and Hodge Jr., P. G., "Elastic-plastic torsion of nonhomogeneous bars by quadratic programming", Int. J. Mech. Sci. Vol.11, pp 53-63(1969)

6. Herakovich, C. T. and Itani, R. Y., "Elastic-plastic torsion of nonhomogeneous bars", J. Eng. Mech. Div. ASCE, pp 757-769(1976)

7. Herrmann, L. R., "Elastic torsional analysis of irregular shapes", J. Eng. Mech. Div. ASCE, Vol.91, pp 11-19(1965)

8. Hodge Jr., P. G., "Elastic-plastic torsion as a problem in non-linear programming", Int. J. Solids Struct. Vol.3, pp 989-999(1967)

9. Klosowicz, B., "On the optimal nonhomogeneity of an elastic bar in torsion;numerical examples", Arch. of Mech., Vol.25, No.6, pp 945-951(1973)

10. Klosowicz, B. and Lurie, K. A., "On the optimal nonhomogeneity of a torsional elastic bar", Arch. of Mech., Vol.24, No.2, pp 239-249(1971)

11. Krahula, J. L., and Lauterbach, G. F., "A finite element solution for Saint-Venant torsion", AIAA J., Vol.7, pp 2200-2203(1969)

12. Love, A. E. H., *A Treatise On The Mechanical Theory Of Elasticity*, 4th edn., Dover, N.Y.(1944)

13. Mazerczyk-Gomulkowa, J. and Mioduchowski, A,, "Optimum plastic nonhomogeneity of a bar subject to torsion with the limit load as a criterion", Bull. Acad. Polon. Sci., Vol.19, No.5, pp 213-220(1971)

14. Mioduchowski, A., "Optimum plastic nonhomogeneity of a bar under torsion as a variational problem", Bull. Acad. Polon. Sci., Vol.29, No.6, pp 253-259(1971)

15. Moan, T., "Finite elemet stress field solution of the problem of Saint-Venent torsion", Int. J. Num. Meth. Eng., Vol.5, pp 455-458(1973)

16. Muskhelishvili, N. I., Some Basic Problems of the Mathematical Theory of Elasticity, N.V.P. Noordhoff, Netherlands(1963)

17. Noor, A. K., and Anderson, C. M., "Mixed isoparametric elements for Saint-Venant torsion", Comput. Meth. Appl. Mech. Eng., Vol.6, pp 195-218(1975)

18. Pian, T. H. H. and Tong, P., "Basis of finite element methods for solid continua", Int. J. for Num. Meth. in Eng. Vol.1, No.1, pp 3-28(1969)

19. Rychlewski, J., "Plastic torsion of a rectangular bar with jump-nonhomogeneity", Int. J. Solids Struct., Vol.1, pp 243-255(1965)

20. Timoshenko, S. and Goodier, J. N., *Theory of Elasticity* McGraw-Hill, N.Y.(1952)

21. Valliappan, S. and Pulamno, V. A., "Torsion of nonhomogeneous anisotropic bars", J. Struct. Div. ASCE, Vol.100, pp 286-295(1974)

22. Yamada, Y., Nakagiri, S. and Takatsuka, K., "Elastic-plastic analysis of Saint-Venant problem by a hybrid stress model", Int. J. Num. Meth. Eng., 5, pp 193-207(1972)

APPENDIX - COMPUTER PROGRAM

```
C     ***************************************************
C
      COMMON TFF(150,30),EFF(3,3,150),EMF(3,150),NP(3,150),
     1 A(3,150),B(3,150),EMM(150),XM(150),YM(150),KOD(150),
     2 IBRY(150),BV(150),MAT(150),TMF(150),G(2),CG1,NECH,
     3 NUMNP,NUMEL,NSEC,NE2M,MBAND,M,MM,NN,PRIG,RIG,TMM,AR
C
      CALL DATA
C
      CALL ASSEMB
C
      KRUN=0
      NECH=5
      DMAX=0.
   10 CALL SOLVE
C
      IF(RIG.LE.PRIG) GO TO 35
      IF(RIG.LE.DMAX) GO TO 36
      DMAX=RIG
      DO 20 I=1,NUMEL
   20 MFIN(I)=MAT(I)
      GO TO 36
   35 IF(NECH.LE.1) GO TO 40
      NECH=NECH-1
   36 PRIG=RIG
      KRUN=KRUN+1
      WRITE(6,2100) KRUN
 2100 FORMAT(/,' NUMBER OF RUN =',I4)
      CALL STRESS
      GO TO 10
C
   40 WRITE(6,2102) (M,MFIN(M),M=1,NUMEL)
 2102 FORMAT(10I6)
      WRITE(6,2103)DMAX
 2103 FORMAT('  MAX. TORSIONAL RIGIDITY =',F10.5)
      STOP
      END
C
C
C     ***************************************************
      SUBROUTINE DATA
C     THIS SUBROUTINE READS AND PRINTS MATERIAL, NODAL AND
C     ELEMENT DATA. IT GENERATES DATA FOR INTERMEDIATE
C     ELEMENTS AND CALCULATES THE BAND WIDTH AND NUMBER OF
C     EQUATIONS.
C     ***************************************************
C
      COMMON TFF(150,30),EFF(3,3,150),EMF(3,150),NP(3,150),
     1 A(3,150),B(3,150),EMM(150),XM(150),YM(150),KOD(150),
     2 IBRY(150),BV(150),MAT(150),TMF(150),G(2),CG1,NECH,
     3 NUMNP,NUMEL,NSEC,NE2M,MBAND,M,MM,NN,PRIG,RIG,TMM,AR
      DIMENSION HED(20),MFIN(150)
```

```
      DIMENSION X(150),Y(150),ISYM(150)
      REAL DN,DX,DY
C
C     BASIC DATA
C
      READ(5,1000) HED,NSEC,NUMEL,NUMNP,NE2M
 1000 FORMAT( 20A4/ 5I6)
      WRITE(6,2000) HED,NSEC,NUMEL,NUMNP,NE2M
 2000 FORMAT(1H1,10X,20A4,////
     1 1H ,  'NUMBER OF SECTIONS      =', I6/
     2 1H ,  'NUMBER OF ELEMENTS      =', I6/
     3 1H ,  'NUMBER OF NODAL POINTS  =', I6/
     4 1H ,  'NO. OF ELEMENTS OF STIFFER MATERIAL  =', I6)
      WRITE(6,2005)
 2005 FORMAT(///,1H ,10X,' MATERIAL PROPERTIES '//
     1 1X,'MAT. NO.',5X, 'SHEAR MODULUS G')
      DO 10 I=1,2
      READ(5,1010) G(I)
 1010 FORMAT(6X,F12.0)
   10 WRITE(6,2010) I,G(I)
 2010 FORMAT (1H ,I5,11X,F10.3)
C
C     NODAL DATA
C
      L=1
      READ(5,1020) N,X(N),Y(N),ISYM(N)
      GO TO 50
   20 READ(5,1020) N,X(N),Y(N),ISYM(N)
 1020 FORMAT(I6,2F12.3,I6)
      DN=N-L
      DX=(X(N)-X(L))/DN
      DY=(Y(N)-Y(L))/DN
   30 L=L+1
      IF(N-L) 60,50,40
   40 X(L)=X(L-1)+DX
      Y(L)=Y(L-1)+DY
      GO TO 30
   50 IF(NUMNP-N) 60,70,20
   60 WRITE(6,2025) N
 2025 FORMAT(1H0,' ERROR IN NODAL DATA,  NODE =',I4)
      CALL EXIT
   70 WRITE(6,2014)
      WRITE(6,2015)
      WRITE(6,2020) (N,X(N),Y(N),N=1,NUMNP)
 2014 FORMAT('1',5X, 'COMPLETE NODAL DATA')
 2015 FORMAT(///,10X,' NODAL POINT OUTPUT',///
     1 1H ,' NODE      X COORD      Y COORD',//)
 2020 FORMAT(I4, 2F12.2)
C
C     ELEMENT DATA
C
      ML=0
   80 IF(ML.GE.NUMEL) GO TO 95
      READ(5,1035) M,NP(1,M),NP(2,M),NP(3,M),IBRY(M)
```

```
 1035 FORMAT(5I6)
      MM=ML+1
      IF(MM.GE.M) GO TO 90
   82 ML1=ML+1
      IF(ML1.GE.M) GO TO 90
      ML2=ML+2
      MM1=ML-1
      IF(MM1.LE.0) GO TO 160
      DO 86 I=1,3
      NP(I,ML2)=NP(I,ML)+1
      NP(I,ML1)=NP(I,MM1)+1
      IBRY(ML2)=IBRY(ML)
      IBRY(ML1)=IBRY(MM1)
   86 CONTINUE
      ML=ML2
      GO TO 82
   90 ML=M
      GO TO 80
C
C     MATERIAL DISTRIBUTION
C
   95 DO 100 K=1,NUMEL
  100 MAT(K)=1
      READ(5,1040) K1,KEL1
      IF(K1.GE.NE2M) GO TO 130
  110 READ(5,1040) K2,KEL2
 1040 FORMAT(2I6)
  120 MAT(KEL1)=2
      K1=K1+1
      KEL1=KEL1+1
      IF(K1.LT.K2) GO TO 120
      KEL1=KEL2
      IF(K2.LT.NE2M) GO TO 110
      MAT(KEL2)=2
      GO TO 140
  130 MAT(KEL1)=2
  140 WRITE(6,2030)
      WRITE(6,2032)
      WRITE(6,2035) (M,(NP(J,M),J=1,3),MAT(M),IBRY(M),
C    1 M=1,NUMEL)
 2030 FORMAT('1',5X,'COMPLETE ELEMENT DATA')
 2032 FORMAT(///,'  ELEM.    I     J     K   MAT.  BDRY')
 2035 FORMAT(6I6)
C
C     BAND WIDTH AND NUMBER OF EQUATIONS
C
      L=0
      DO 150 M=1,NUMEL
      DO 150 I=1,2
      I1=I+1
      DO 150 J=I1,3
      K=IABS(NP(I,M)-NP(J,M))
      IF(K.GT.L) L=K
  150 CONTINUE
```

```
      MBAND=L+1
      NEQ=NUMNP
      WRITE(6,2040) MBAND,NEQ
      IF(MBAND.LE.40.AND.NEQ.LE.150) GO TO 170
      WRITE(6,2050)
 2040 FORMAT(///,10X, 'BAND WIDTH           =',I6/
     1           10X, 'NUMBER OF EQUATIONS =',I6)
 2050 FORMAT(///,10X,' PROBLEM EXCEEDS SPECIFIED LIMITS')
      CALL EXIT
  160 WRITE(6,2060)
 2060 FORMAT(///,' MM1 IS LESS THAN OR EQUAL TO ZERO')
      CALL EXIT
  165 WRITE(6,2095) M
 2095 FORMAT(1H ,'NEGATIVE AREA ELEMENT=',I6)
      CALL EXIT
  170 IF(NSEC.LE.1)GO TO 190
      MM=0
      NR=0
C
C     NODES ON THE BOUNDARY OF SECTIONS
C
      DO 180 I=1,NUMNP
      IF(ISYM(I).EQ.1) GO TO 180
      NR=NR+1
      KOD(NR)=I
  180 CONTINUE
      NN=NR
      RETURN
  190 MM=MBAND
      NN=NEQ-1
      RETURN
      END
C
C     ***************************************************
      SUBROUTINE ASSEMB
C     THIS SUBROUTINE TAKES EACH ELEMENT IN TURN AND FORMS
C     THE ELEMENT STIFFNESS MATRIX AND ASSEMBLES THE GLOBAL
C     STIFFNESS MATRIX.
C     ***************************************************
C
      COMMON TFF(150,30),EFF(3,3,150),EMF(3,150),NP(3,150),
     1 A(3,150),B(3,150),EMM(150),XM(150),YM(150),KOD(150),
     2 IBRY(150),BV(150),MAT(150),TMF(150),G(2),CG1,NECH,
     3 NUMNP,NUMEL,NSEC,NE2M,MBAND,M,MM,NN,PRIG,RIG,TMM,AR
C
C     INITIALIZE
C
      DO 10 I=1,NUMNP
      TMF(I)=0.0
      DO 10 J=1,MBAND
      TFF(I,J)=0.0
   10 CONTINUE
      TMM=0.0
C
```

```
C       ELEMENT STIFFNESS MATRICES
C
        AR=(A(3,1)*B(2,1)-A(2,1)*B(3,1))/2.0
        CG=G(2)/G(1)
        CG1=CG-1
        GV=G(1)
        C1=GV/2.
        C2=GV/(4.*AR)
        DO 70 M=1,NUMEL
        I=NP(1,M)
        J=NP(2,M)
        K=NP(3,M)
        A(1,M)=X(K)-X(J)
        A(2,M)=X(I)-X(K)
        A(3,M)=X(J)-X(I)
        B(1,M)=Y(J)-Y(K)
        B(2,M)=Y(K)-Y(I)
        B(3,M)=Y(I)-Y(J)
        XO=(X(I)+X(J)+X(K))/3.0
        YO=(Y(I)+Y(J)+Y(K))/3.0
        XM(M)=XO
        YM(M)=YO
        AI=A(1,M)
        BI=B(1,M)
        IF(IBRY(M).GT.0) GO TO 30
C
C       (1) INNER ELEMENTS
C
        AJ=A(2,M)
        AK=A(3,M)
        BJ=B(2,M)
        BK=B(3,M)
        EMM(M)=GV*AR*(XO*XO+YO*YO)
        EMF(1,M)=C1*(AI*XO-BI*YO)
        EMF(2,M)=C1*(AJ*XO-BJ*YO)
        EMF(3,M)=C1*(AK*XO-BK*YO)
        EFF(1,1,M)=C2*(AI*AI+BI*BI)
        EFF(1,2,M)=C2*(AI*AJ+BI*BJ)
        EFF(1,3,M)=C2*(AI*AK+BI*BK)
        EFF(2,1,M)=EFF(1,2,M)
        EFF(2,2,M)=C2*(AJ*AJ+BJ*BJ)
        EFF(2,3,M)=C2*(AJ*AK+BJ*BK)
        EFF(3,1,M)=EFF(1,3,M)
        EFF(3,2,M)=EFF(2,3,M)
        EFF(3,3,M)=C2*(AK*AK+BK*BK)
        GO TO 40
C
C       (2) BOUNDARY ELEMENTS
C
   30   SL23=AI*AI+BI*BI
        EK=GV*AR/SL23
        EM=YO*AI+XO*BI
        EMM(M)=EK*EM**2
        EMF(2,M)=EM*EK
```

```
      EMF(3,M)=-EM*EK
      EFF(2,2,M)=EK
      EFF(2,3,M)=-EK
      EFF(3,2,M)=-EK
      EFF(3,3,M)=EK
C
C     GLOBAL STIFFNESS MATRIX
C
   40 IF(MAT(M).GE.2) GO TO 47
      TMM=TMM+EMM(M)
      KI=1
      IF(IBRY(M).GT.0) KI=2
      DO 46 I=KI,3
      II=NP(I,M)
      TMF(II)=EMF(I,M)+TMF(II)
      DO 44 J=KI,3
      JJ=NP(J,M)-II+1
      IF(JJ.LE.0) GO TO 44
      TFF(II,JJ)=TFF(II,JJ)+EFF(I,J,M)
   44 CONTINUE
   46 CONTINUE
      GO TO 70
   47 TMM=TMM+CG*EMM(M)
      KI=1
      IF(IBRY(M).GT.0) KI=2
      DO 49 I=KI,3
      II=NP(I,M)
      TMF(II)=CG*EMF(I,M)+TMF(II)
      DO 48 J=KI,3
      JJ=NP(J,M)-II+1
      IF(JJ.LE.0) GO TO 48
      TFF(II,JJ)=TFF(II,JJ)+CG*EFF(I,J,M)
   48 CONTINUE
   49 CONTINUE
   70 CONTINUE
      RETURN
 2150 FORMAT(10F7.3)
      END
C
C     ***************************************************
      SUBROUTINE SOLVE
C     THIS SUBROUTINE SOLVES THE SET OF EQUATIONS FOR
C     THE VALUES OF WARPING FUNCTION AT THE NODAL POINTS
C     AND CALCULATES THE TORSIONAL RIGIDITY.
C     ***************************************************
C
      COMMON TFF(150,30),EFF(3,3,150),EMF(3,150),NP(3,150),
     1 A(3,150),B(3,150),EMM(150),XM(150),YM(150),KOD(150),
     2 IBRY(150),BV(150),MAT(150),TMF(150),G(2),CG1,NECH,
     3 NUMNP,NUMEL,NSEC,NE2M,MBAND,M,MM,NN,PRIG,RIG,TMM,AR
      DIMENSION AM(150,30)
      IF(NSEC.LE.1) GO TO 16
      IF(MM.GT.0) GO TO 10
      DO 3 I=1,NN
```

```
      DO 3 J=1,MBAND
    3 AM(I,J)=0.0
      I=0
    4 I=I+1
      IF(I.GT.NN) GO TO 14
      II=KOD(I)
      BV(I)=-TMF(II)
      KOUNT=0
      J=I-1
    5 J=J+1
      JJ=KOD(J)-II+1
      IF(JJ.GT.MBAND) GO TO 4
      L=J-I+1
      KOUNT=KOUNT+1
      AM(I,L)=TFF(II,JJ)
      IF(MM.LT.KOUNT) MM=KOUNT
      IF(J.LT.NN) GO TO 5
    7 I=I+1
      IF(I.GT.NN) GO TO 14
      II=KOD(I)
      BV(I)=-TMF(II)
      DO 8 J=I,NN
      JJ=KOD(J)-II+1
      IF(JJ.GT.MBAND) GO TO 9
      L=J-I+1
    8 AM(I,L)=TFF(II,JJ)
    9 GO TO 7
   10 NL=NN-MM+1
      DO 12 I=1,NN
      II=KOD(I)
      BV(I)=-TMF(II)
      DO 11 J=I,NN
      L=J-I+1
      IF(L.GT.MM) GO TO 12
      JJ=KOD(J)-II+1
      IF(JJ.GT.MBAND) GO TO 12
   11 AM(I,L)=TFF(II,JJ)
   12 CONTINUE
   14 NL=NN-MM+1
      NM=NN-1
      IF(NM) 110,90,30
   16 NL=NN-MM+1
      NM=NN-1
C
C     STORE TFF AND TMF IN AM AND BV AND APPLY DISPLACEMENT
C     BOUNDARY CONDITION.
C
      DO 18 K=1,NN
      K1=K+1
   18 BV(K)=-TMF(K1)
      DO 20 J=1,MM
      DO 20 I=1,NN
      I1=I+1
   20 AM(I,J)=TFF(I1,J)
```

```
C
C       TRIANGULARIZE AM AND REDUCE BV
C
   30 MR=MM
      DO 52 N=1,NM
      IF(AM(N,1).GT.0.0001) GO TO 35
      AM(N,1)=1.
      BV(N)=0.
      DO 32 KC=2,MM
   32 AM(N,KC)=0.
      GO TO 52
   35 BN=BV(N)
      BV(N)=BN/AM(N,1)
      IF(N.GT.NL) MR=NN-N+1
      DO 50 L=2,MR
      IF(AM(N,L).EQ.0.0) GO TO 50
      C=AM(N,L)/AM(N,1)
      I=N+L-1
      J=0
      DO 40 K=L,MR
      J=J+1
   40 AM(I,J)=AM(I,J)-C*AM(N,K)
      BV(I)=BV(I)-C*BN
      AM(N,L)=C
   50 CONTINUE
   52 CONTINUE
C
C       BACK SUBSTITUTE
C
      I=NN
   55 BV(NN)=BV(NN)/AM(NN,1)
      DO 60 N=1,NM
      I=I-1
      IF(N.LT.MM) MR=N+1
      DO 60 J=2,MR
      K=I+J-1
   60 BV(I)=BV(I)-AM(I,J)*BV(K)
C
C       TORSIONAL RIGIDITY
C
      T=0.0
      IF(NSEC.GT.1) GO TO 82
   70 DO 80 II=1,NN
      IJ=II+1
      T=T+TMF(IJ)*BV(II)
   80 CONTINUE
      GO TO 88
   82 DO 85 II=1,NN
      IJ=KOD(II)
   85 T=T+TMF(IJ)*BV(II)
   88 RIG=(TMM+T)*NSEC
      WRITE(6,2070) RIG
      RETURN
   90 BV(1)=BV(1)/AM(1,1)
```

```
      JP=KOD(1)
      RIG=(TMM+TMF(JP)*BV(1))*NSEC
      WRITE(6,2070) RIG
 2070 FORMAT(///,'TORSIONAL RIGIDITY =',F12.6)
      RETURN
  110 WRITE(6,3010)
 3010 FORMAT('ELEMENTS ARE NOT DIVIDED PROPERLY')
      CALL EXIT
 3000 FORMAT(1H ,'ZERO OR NEGATIVE ELEMENT ON MAIN DIAGONAL
     1 OF TRIANGULARIZED MATRIX', I5)
      END
C
C     ***************************************************
      SUBROUTINE STRESS
C     THIS SUBROUTINE COMPUTES STRESSES IN EVERY ELEMENTS,
C     COMPARE THEIR MAGNITUDES, SELECT PAIRS OF ELEMENTS
C     FOR INTERCHANGE AND MODIFY THE STIFFNESS MATRIX.
C     ***************************************************
C
      COMMON TFF(150,30),EFF(3,3,150),EMF(3,150),NP(3,150),
     1 A(3,150),B(3,150),EMM(150),XM(150),YM(150),KOD(150),
     2 IBRY(150),BV(150),MAT(150),TMF(150),G(2),CG1,NECH,
     3 NUMNP,NUMEL,NSEC,NE2M,MBAND,M,MM,NN,PRIG,RIG,TMM,AR
      DIMENSION W(150),SQT(150)
      DO 10 I=1,NUMNP
   10 W(I)=0.
      IF(NSEC.LE.1) GO TO 30
      DO 20 J=1,NN
      KP=KOD(J)
   20 W(KP)=BV(J)
      GO TO 40
C
C     SHEAR STRESSES
C
   30 DO 35 J=1,NN
      J1=J+1
   35 W(J1)=BV(J)
   40 DO 60 K=1,NUMEL
      I1=NP(1,K)
      I2=NP(2,K)
      I3=NP(3,K)
      IF(IBRY(K).NE.0) GO TO 50
      TXZ=(-YM(K)+(B(1,K)*W(I1)+B(2,K)*W(I2)+B(3,K)*W(I3))/
     1 (2.*AR))
      TYZ=(XM(K)+(A(1,K)*W(I1)+A(2,K)*W(I2)+A(3,K)*W(I3))/
     1 (2.*AR))
      GO TO 55
   50 AK=A(1,K)
      BK=B(1,K)
      SL23=AK*AK+BK*BK
      TXZ=(AK/SL23)*(-AK*YM(K)-BK*XM(K)-W(I2)+W(I3))
      TYZ=(BK/SL23)*(AK*YM(K)-BK*XM(K)+W(I2)-W(I3))
   55 SQT(K)=TXZ*TXZ+TYZ*TYZ
   60 CONTINUE
```

```
C
C     SELECT PAIRS OF ELEMENTS
C
      KAL=1
   65 TMIN=SQT(1)
      TMAX=TMIN
      NDN=1
      NUP=1
   70 DO 80 M=2,NUMEL
      IF(MAT(M).GE.2) GO TO 75
      IF(SQT(M).LE.TMAX) GO TO 80
      TMAX=SQT(M)
      NUP=M
      GO TO 80
   75 IF(SQT(M).GE.TMIN) GO TO 80
      TMIN=SQT(M)
      NDN=M
   80 CONTINUE
      IF(TMIN.GE.TMAX) GO TO 100
      KI=1
      MAT(NUP)=2
      MAT(NDN)=1
      IF(IBRY(NUP).NE.0) KI=2
C
C     MODIFY THE SET OF EQUATIONS
C
      DO 95 I=KI,3
      II=NP(I,NUP)
      TMF(II)=TMF(II)+CG1*EMF(I,NUP)
      DO 93 J=KI,3
      JJ=NP(J,NUP)-II+1
      IF(JJ.LE.0) GO TO 93
      TFF(II,JJ)=TFF(II,JJ)+CG1*EFF(I,J,NUP)
   93 CONTINUE
   95 CONTINUE
      KI=1
      IF(IBRY(NDN).NE.0) KI=2
      DO 99 I=KI,3
      II=NP(I,NDN)
      TMF(II)=TMF(II)-CG1*EMF(I,NDN)
      DO 94 J=KI,3
      JJ=NP(J,NDN)-II+1
      IF(JJ.LE.0) GO TO 94
      TFF(II,JJ)=TFF(II,JJ)-CG1*EFF(I,J,NDN)
   94 CONTINUE
   99 CONTINUE
      TMM=TMM+CG1*(EMM(NUP)-EMM(NDN))
      WRITE(6,2805) NDN,NUP
      IF(KAL.GE.NECH) GO TO 100
      KAL=KAL+1
 2805 FORMAT('ELEMENT CHANGED #',I6,'  AND #',I6)
      GO TO 65
  100 RETURN
      END
```